Heavy fermions in high magnetic field

Alix McCollam

High Field Magnet Laboratory (HFML), Nijmegen, The Netherlands.

Outline

- Introduction to heavy fermion systems (via key experimental quantities)
- Measuring heavy fermions in high magnetic fields
- Quantum criticality (brief)
- High field behaviour of $Ce_nT_mIn_{3n+2m}$ (focusing on $CePt_2In_7$)

f-electrons

4*f*	Ce 58 140.12 Cerium	Pr 59 140.91 Praseodymium	Nd 60 144.24 Neodymium	Pm 61 (145) Promethium	Sm 62 150.36 Samarium	Eu 63 152.97 Europium	Gd 64 157.25 Gadolinium	Tb 65 158.93 Terbium	Dy 66 162.50 Dysprosium	Ho 67 164.93 Holmium	Er 68 167.26 Erbium	Tm 69 168.93 Thulium	Yb 70 173.04 Ytterbium	Lu 71 174.97 Lutetium
5*f*	Th 90 232.04 Thorium	Pa 91 231.04 Protactinium	U 92 238.03 Uranium	Np 93 237.05 Neptunium	Pu 94 (240) Plutonium	Am 95 243.06 Americium	Cm 96 (247) Curium	Bk 97 (248) Berkelium	Cf 98 (251) Californium	Es 99 252.08 Einsteinium	Fm 100 257.10 Fermium	Md 101 (257) Mendelevium	No 102 259.10 Nobelium	Lr 103 262.11 Lawrencium

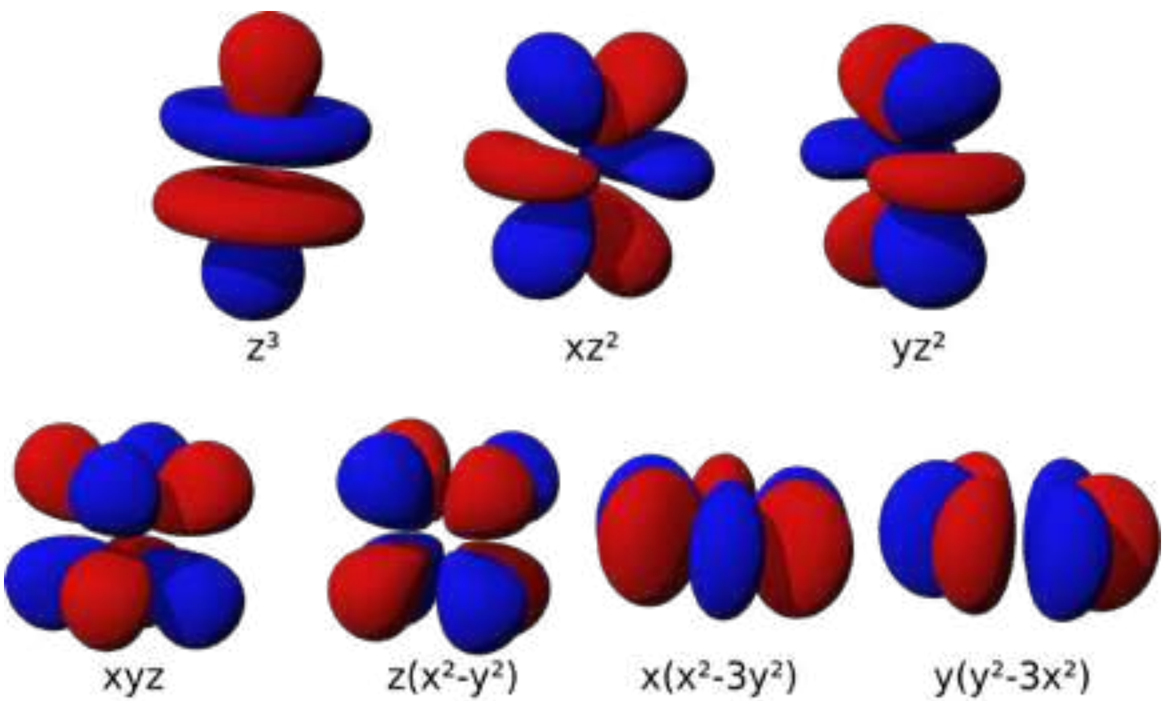

Ce: $4f^{1}\,5d^{1}\,6s^{2}$

Pr: $4f^{2}\,5d^{1}\,6s^{2}$ (solid)

Yb: $4f^{13}5d^{1}\,6s^{2}$

U: $5f^{3}\,6d^{1}\,7s^{2}$

Np: $5f^{3}\,6d^{1}7s^{2}$

Heavy fermions

Classic symptoms.

At low temperature...

large specific heat: $$C(T) = \gamma\, T + \beta\, T^3\ (+\, C_{\text{spin fluctuations}})$$

large *m** in de Haas-van Alphen experiments: $$R(T) = \frac{(2\pi^2 k_B T m^*/\hbar e B)}{\sinh(2\pi^2 k_B T m^*/\hbar e B)}$$

large *A* coefficient of T^2 resistivity: $$\rho(T) \sim \rho_0 + A\, T^2$$

large magnetic susceptibility, sometimes saturated: $$\chi_{\text{Pauli}} \sim N(\varepsilon_F)$$
(Curie-Weiss at high *T*)

(Thermal conductivity: $$\kappa(T) \sim C(T)$$
and related quantities)

Specific heat

$$\frac{C}{T} = \gamma + \beta\, T^2$$

For free electrons

$$\gamma = \frac{\pi^2}{3} k_B^2 N_F = \frac{k_B^2}{3\hbar^2} k_F m^*$$

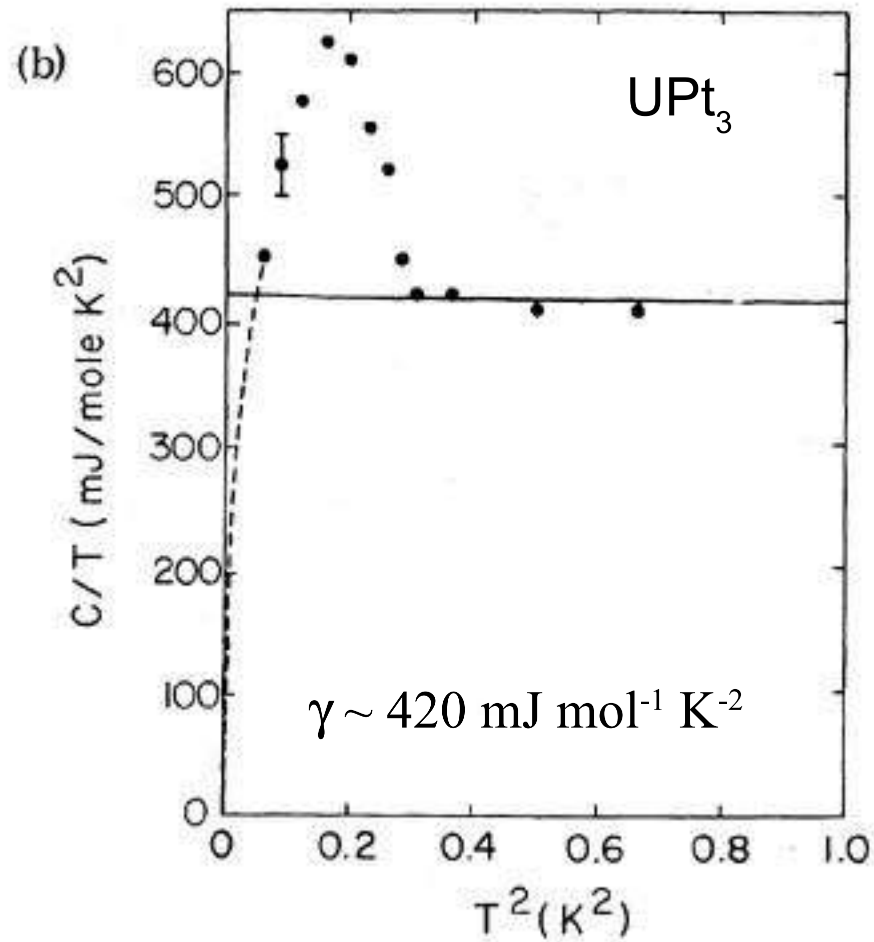

Compare $\gamma \sim 1.2$ mJ mol^{-1} K^{-2} for aluminium.

Stewart *et al*. PRL **52**, 679 (1984)

Magnetic susceptibility

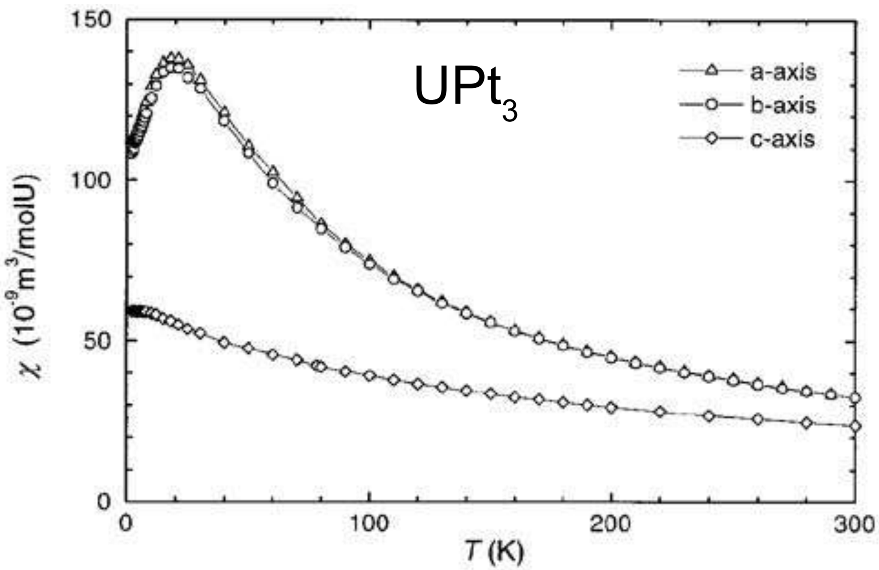

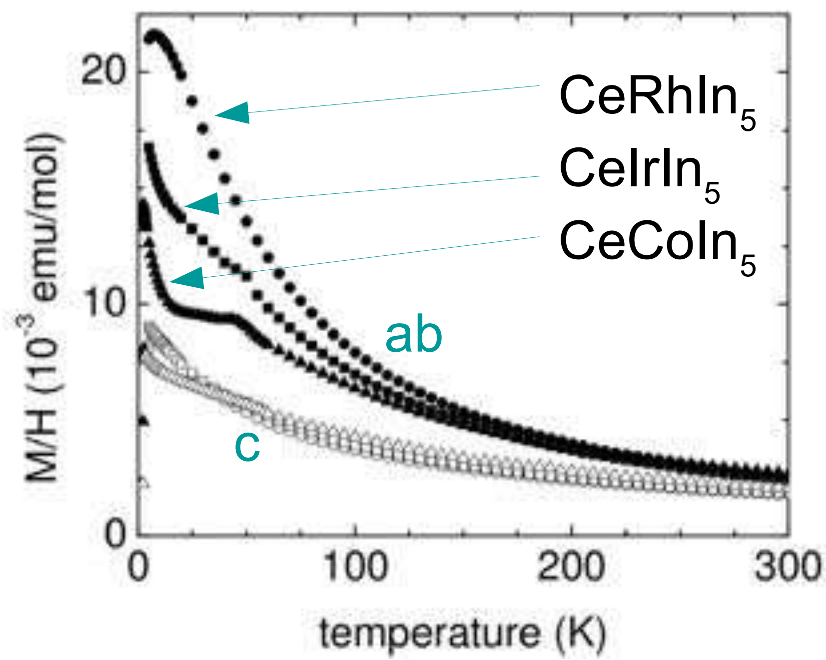

Low T: $\chi_{\mathrm{Pauli}} \sim N(\varepsilon_F)$

χ_{vv}

High T: $\chi_{\mathrm{cw}} \approx n \dfrac{M^2}{3(T+\theta)}$

Frings *et al*. J. Magn. Magn. Mater **31-34**, 240 (1983)

Petrovic *et al.* J. Phys.Condens.Matter **13,** L337 (2001)

Electrical resistivity

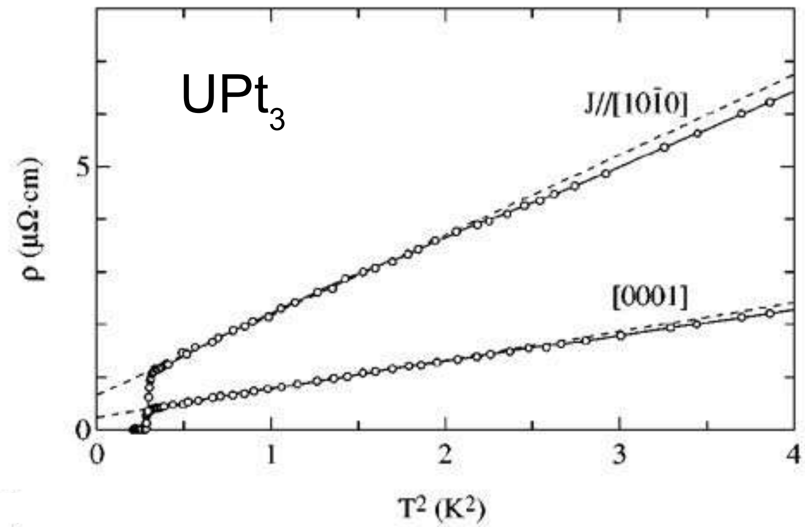

$$\rho(T) \sim \rho_0 + A\, T^2$$

$A_{1010} \sim 1.55 \pm 0.1\ \mu\Omega$ cm K^{-2}

$A_{0001} \sim 0.55 \pm 0.05\ \mu\Omega$ cm K^{-2}

Kadowaki-Woods ratio: $\gamma \sim \sqrt{A}$

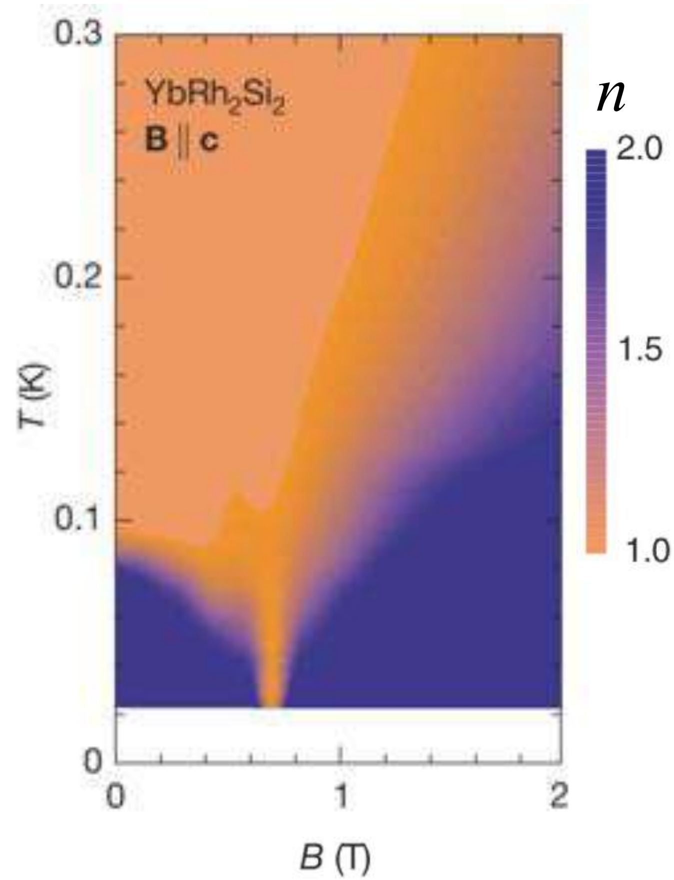

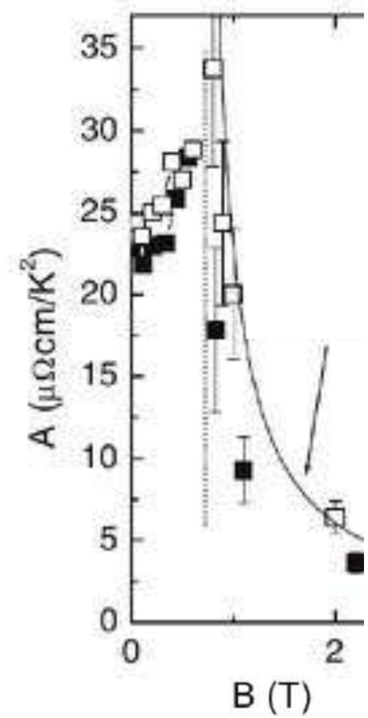

$$\rho(T) \sim \rho_0 + A\, T^n$$

Kimura *et al*. JPSJ **64**, 3881 (1995)

Gegenwart *et al*. PRL **89**, 056402 (2002)

Custers *et al*. Nature **424**, 524 (2003)

Local *f*-moments

A system of local moments has a Curie susceptibility

$$\chi = \frac{\partial M}{\partial B} = \frac{\mu_B^2}{T}$$

$$\mathbf{M} = \mu_B \, \boldsymbol{\sigma}$$

Typical signature is the appearance of Curie paramagnetism, with high temperature Curie-Weiss magnetic susceptibility:

$$\chi_{\rm cw} \approx n \frac{M^2}{3(T+\theta)}$$

$$M^2 = g^2 \mu_B^2 \; J(J+1)$$

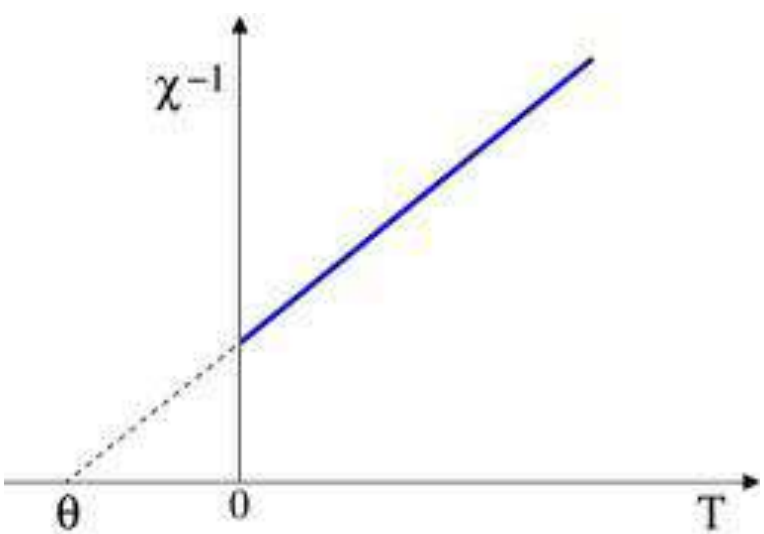

n concentration of magnetic moments

M magnetic moment with total angular momentum quantum number *J*

θ Curie-Weiss temperature

The Kondo effect (single impurity)

Conduction electrons and local moment interact via an antiferromagnetic contact interaction of strength *J.*

$$J \quad \rightarrow \quad J(T) = J + 2J^2\rho \;\ln\frac{D}{T}$$

ρ d.o.s of conduction sea per spin
D bandwidth

When temperature becomes of order $T_K \;\sim\; D\;\exp\left(-\frac{1}{2J\rho}\right)$

the second term becomes as big as the first.

$T < T_K$: Kondo coupling is strong
conduction electrons magnetically screen the local moment
bound singlet state is formed

Electron fluid surrounding the Kondo singlet is a Fermi liquid with χ_{Pauli}

Characteristic zero temperature specific heat co-efficient is of order

$$\gamma = \frac{C}{T}\;(T \rightarrow 0) \;\sim\; \frac{R\ln 2}{T_K}$$

Local moments on a lattice

c - *f* electron hybridisation: constant exchange spin-flip transitions of *f*-electrons and conduction electrons near ε_F

$$e^-_\downarrow + f^1_\uparrow \rightleftharpoons e^-_\uparrow + f^1_\downarrow$$

Rate τ^{-1} defines the temperature scale $$k_B T_K = \frac{\hbar}{\tau}$$

On a lattice, the Kondo effect develops coherence

Single impurity Kondo singlet scatters electrons without conserving momentum

→ increase of resistivity at low *T*

Crystal lattice has translational symmetry; the same elastic scattering now conserves momentum

→ (phase) coherent scattering off the Kondo singlets leads to reduction of resistivity at $T < T_K$.

Coherence on the Kondo lattice

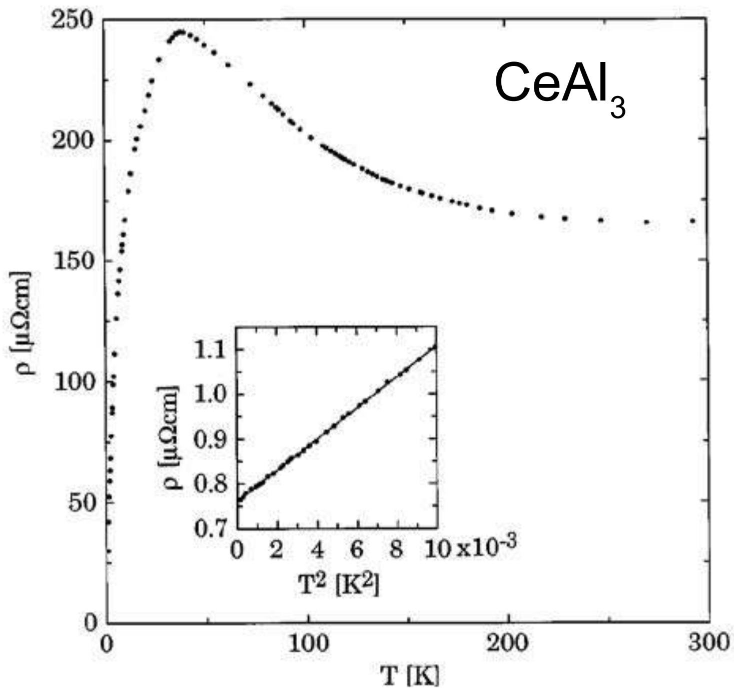

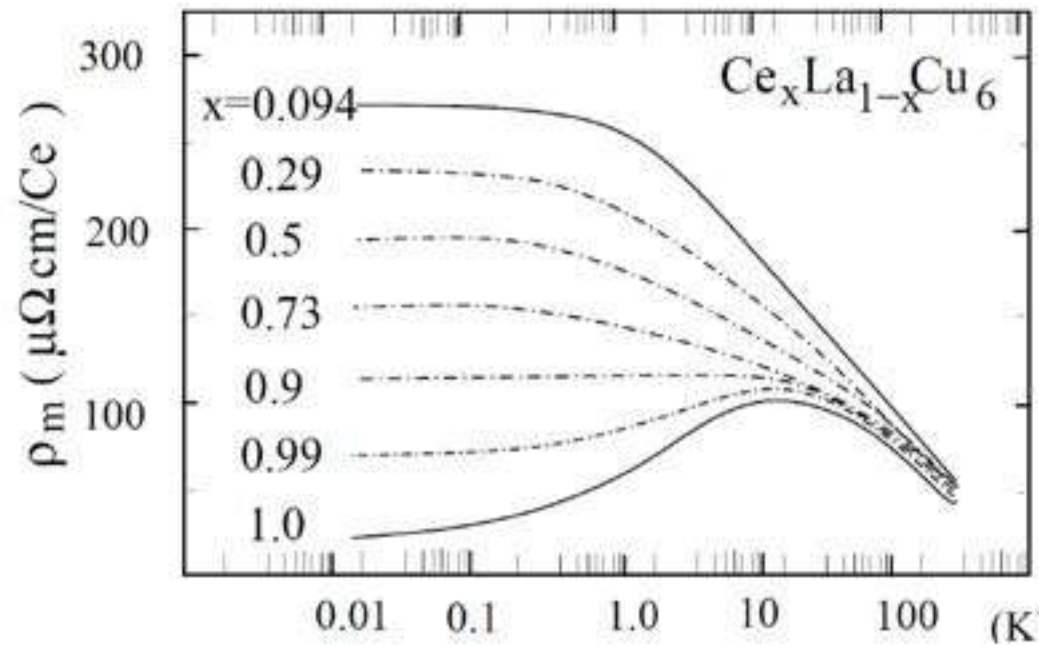

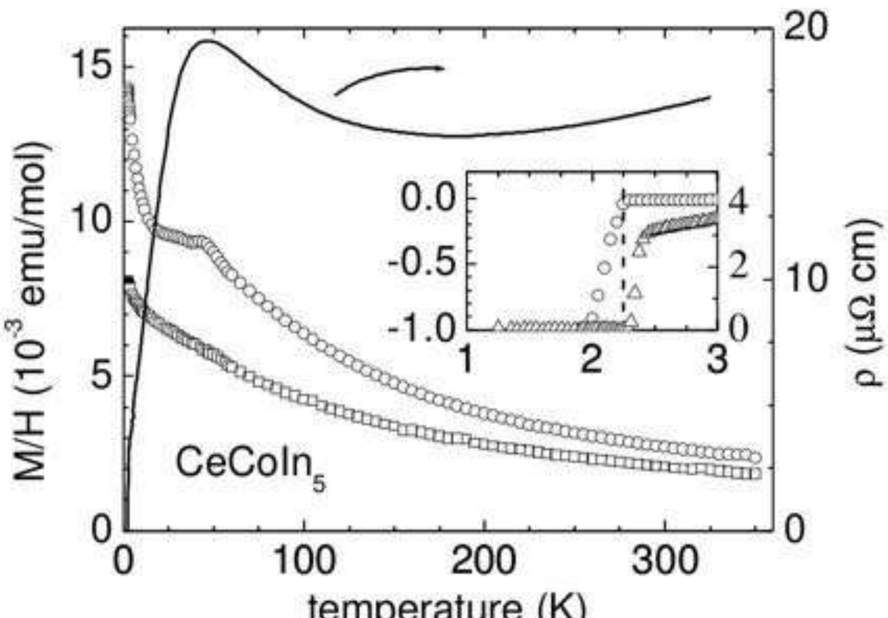

Andres *et al.* PRL **35,** 1779 (1975)

Petrovic *et al.* J. Phys.Condens.Matter **13,** L337 (2001)

Onuki and Komatsubara,
J. Magn. Magn. Mater **63-64**, 281 (1987)

Renormalised density of states

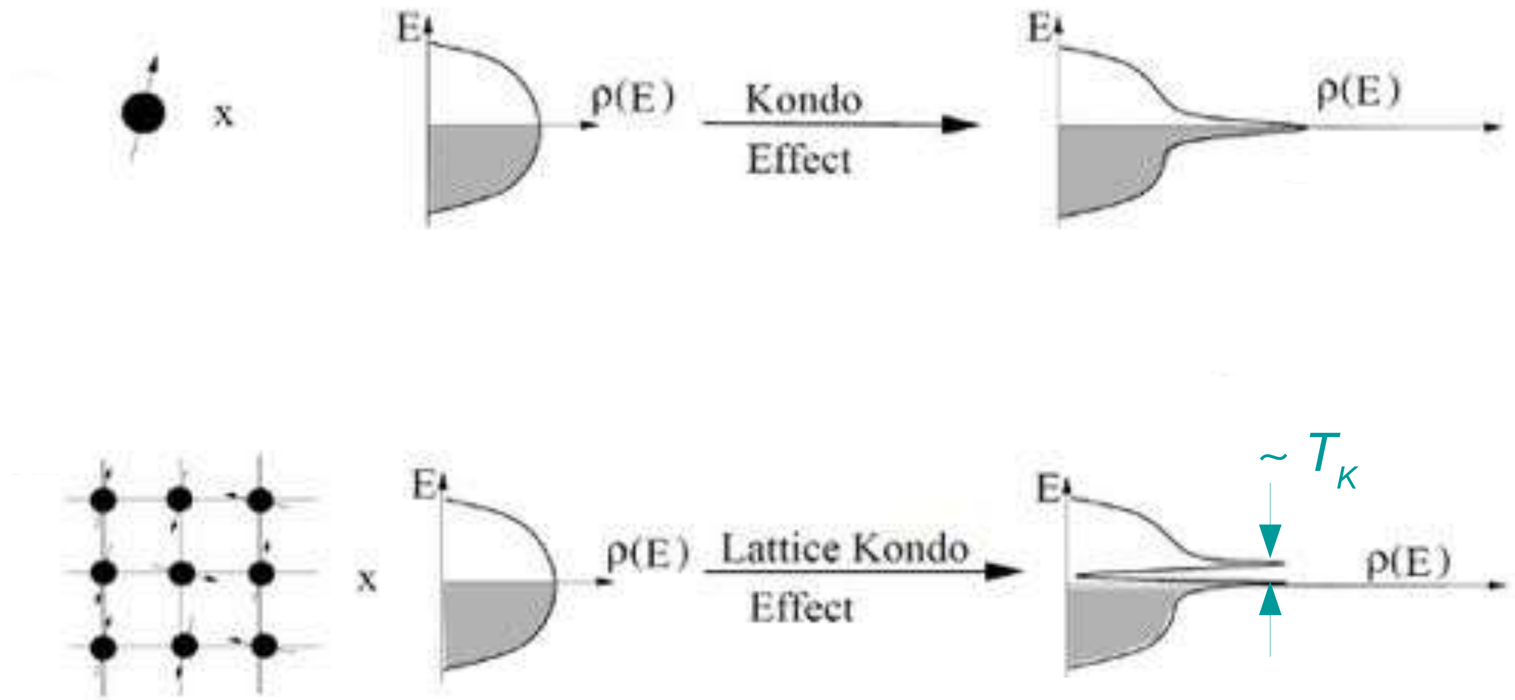

Lattice Kondo effect builds a fermionic resonance into the conduction sea in each unit cell.

The elastic scattering off this lattice of resonances leads to formation of a heavy fermion band, of width T_K.

Renormalised bandstructure

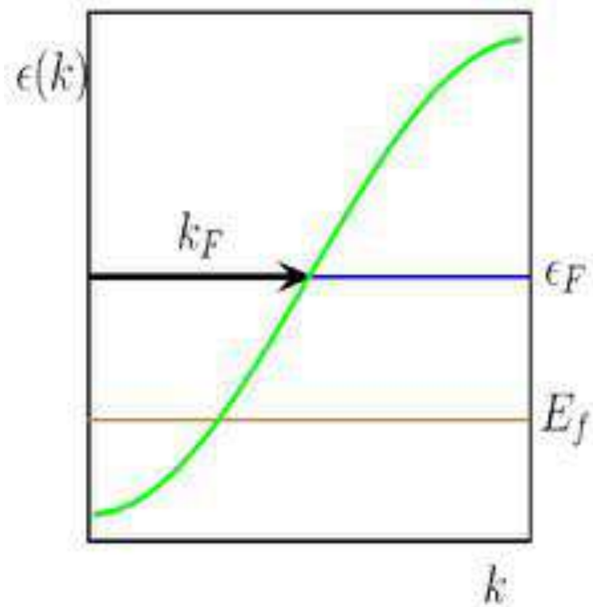

f-levels lie close to the Fermi energy

The conduction band is reconstructed due to c-*f* hybridisation

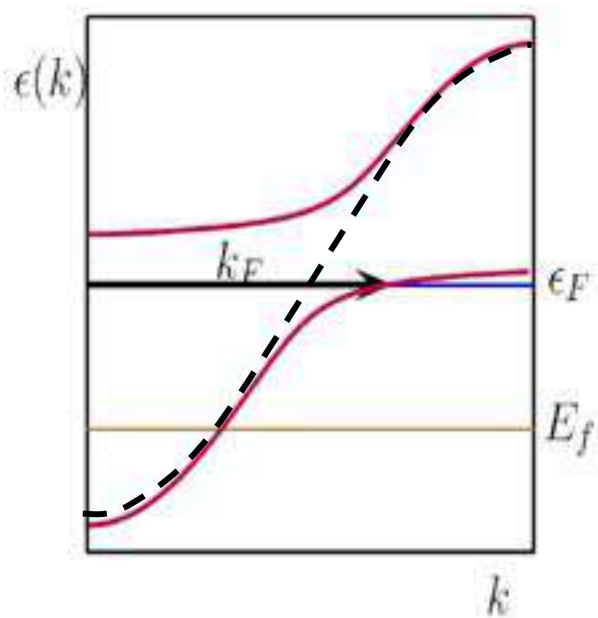

The Fermi surface changes from “small” to “large”.

Millis, Lavagna and Lee, PRB **36**, 864 (1987)

Local moment antiferromagnetism (RKKY)

When J is weak:

Local f-moments polarise the conduction electron sea, giving rise to Friedel oscillations in the magnetisation

Leads to antiferromagnetic (indirect exchange) interaction between local moments

$\rightarrow$ tends to order

RKKY interaction

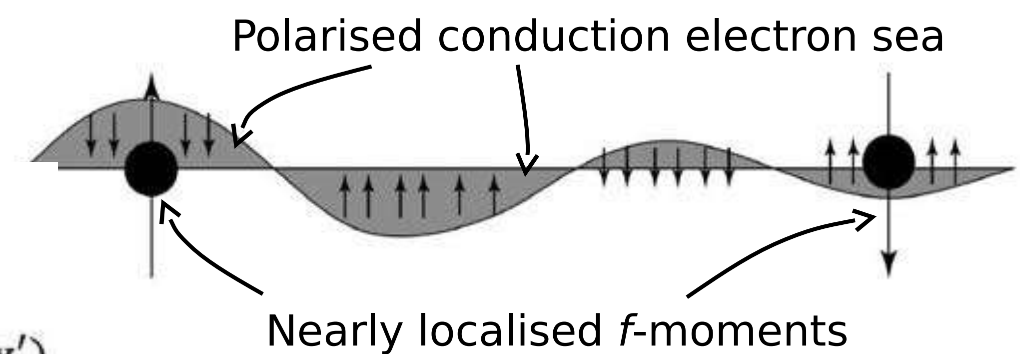

$$H_{RKKY} = \frac{1}{2}\sum_{\mathbf{x},\mathbf{x}'} \overbrace{-J^2\chi(\mathbf{x}-\mathbf{x}')}^{J_{RKKY}(\mathbf{x}-\mathbf{x}')}\,\mathbf{S}(\mathbf{x})\cdot\mathbf{S}(\mathbf{x}')$$

$$J_{RKKY}(r) \sim J^2 \rho \frac{\cos 2k_F r}{|r|^3}$$

- J strength of Kondo coupling
- ρ conduction electron d.o.s. per spin
- r distance from local moment
- χ non-local susceptibility

P. Coleman, *Introduction to many body physics.* CUP.

Fermions can still be heavy

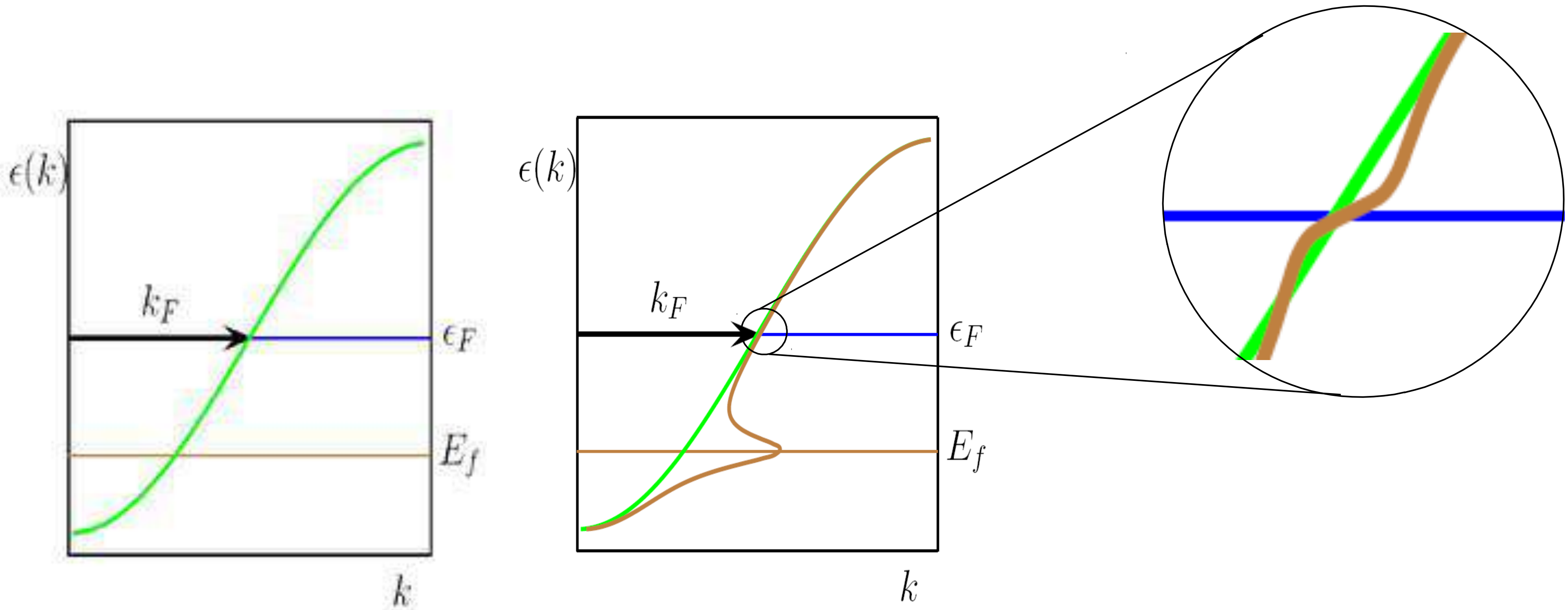

Sigma-shaped distortion of the conduction band due to interaction between local moments and spin fluctuations in conduction electron sea.

Flattening of the band at the Fermi energy leads to heavy masses, but Fermi surface remains "small".

Auerbach and Levin,
J. Appl. Phys. **61**, 3162 (1987)

"Standard model": competing energy scales

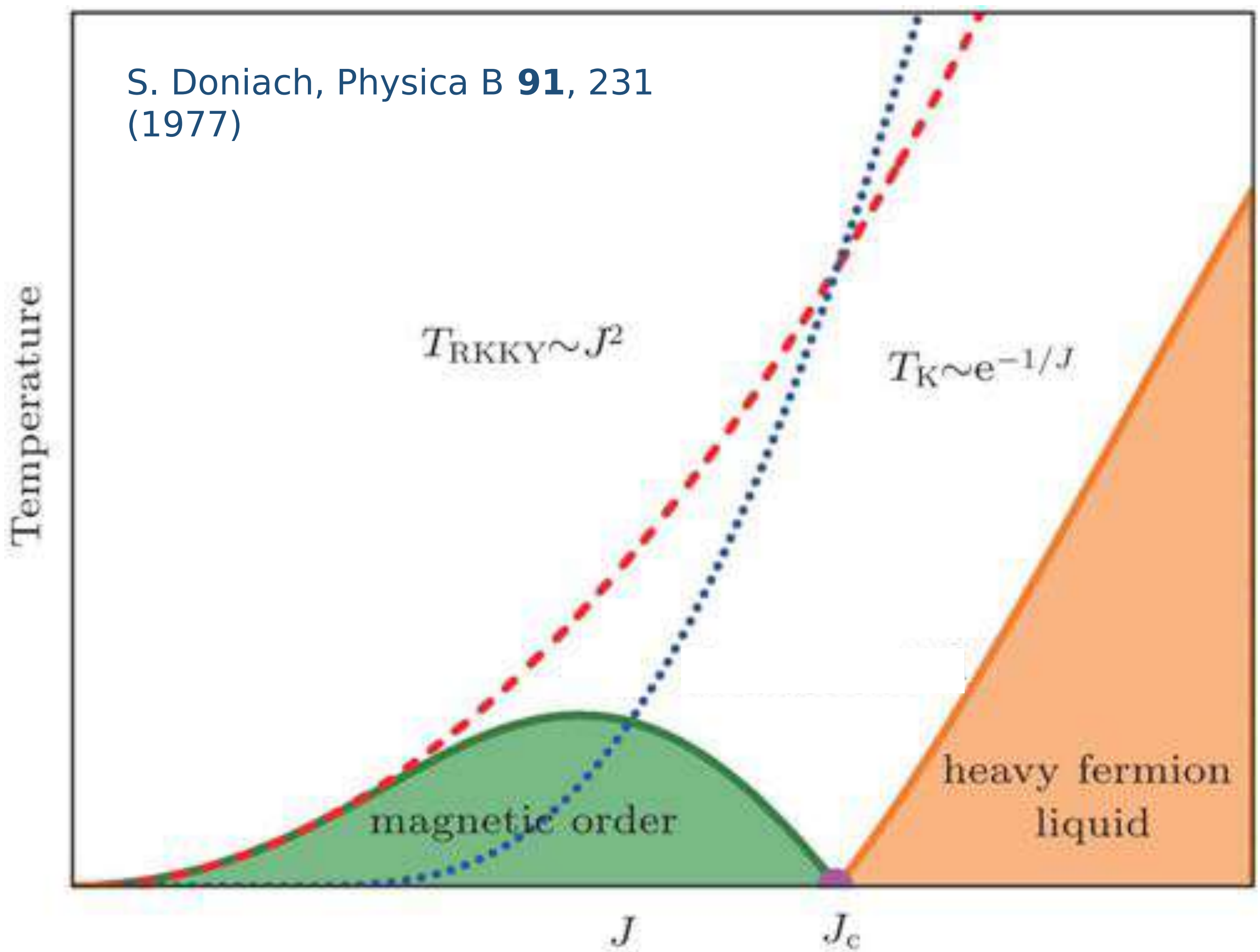

Small J: $E_{RKKY} >> T_K$ AFM

Large J: $T_K >> E_{RKKY}$ "heavy fermions"

Transition between AFM and the dense Kondo ground state is a continuous quantum phase transition.

HFs are highly tunable

Spin, charge and lattice/orbital degrees of freedom are all strongly coupled. Changing one has a significant effect on the others.

Combine this with the RKKY vs. Kondo competition, and the fine balance of energies and interactions leads to very complex phase diagrams.

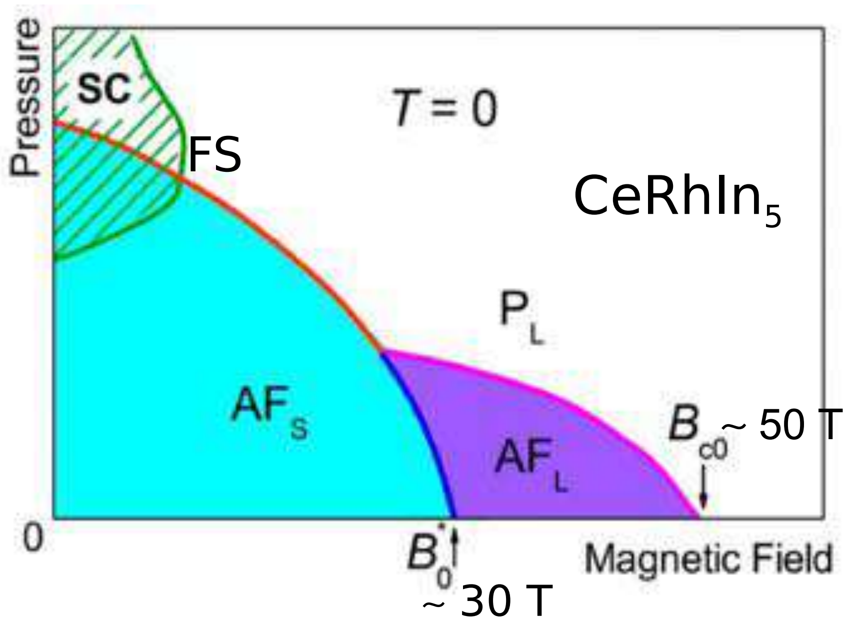

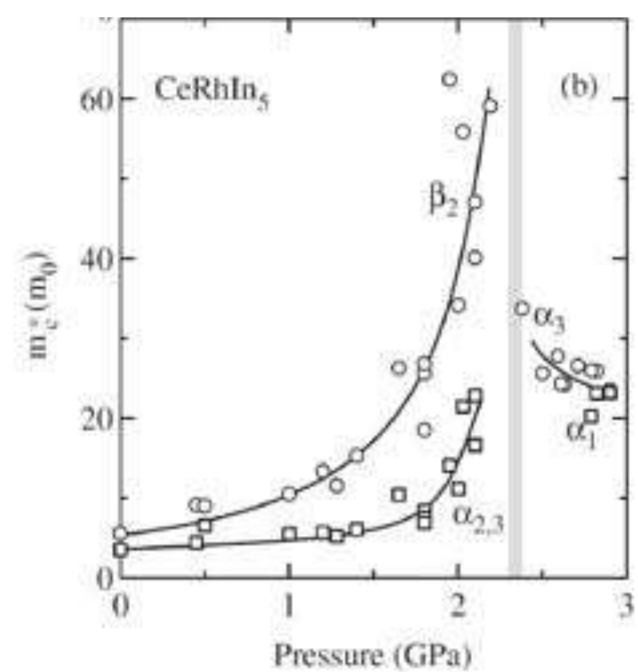

"Some are born heavy, some achieve heaviness, and some have heaviness thrust upon them".

William Shakespeare
(Twelfth Night)

Shishido *et al*., JPSJ **74,** 1103 (2005)
Knebel *et al*., PRB **74**, 020501(R) (2006)
Jiao *et al*., PNAS **112**, 673 (2015)

Historically....

Fig. 2 – De Haas and the large magnet.

"Together with the famous cryogenic apparatus, it is an unequalled equipment to study magnetism at low temperature."

W.J. de Haas (1878-1960)

Quantum criticality in HFs

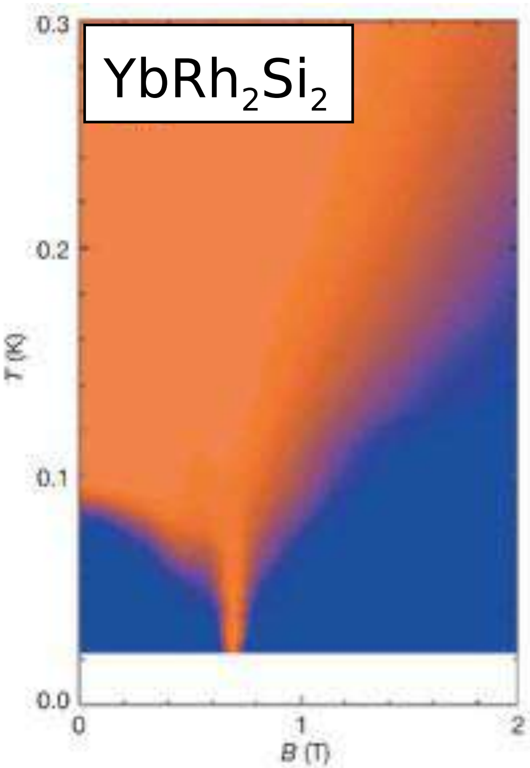

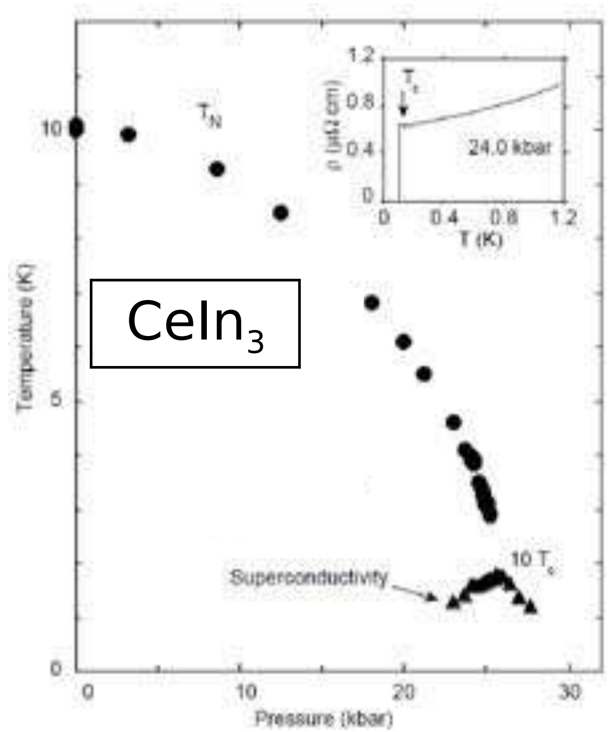

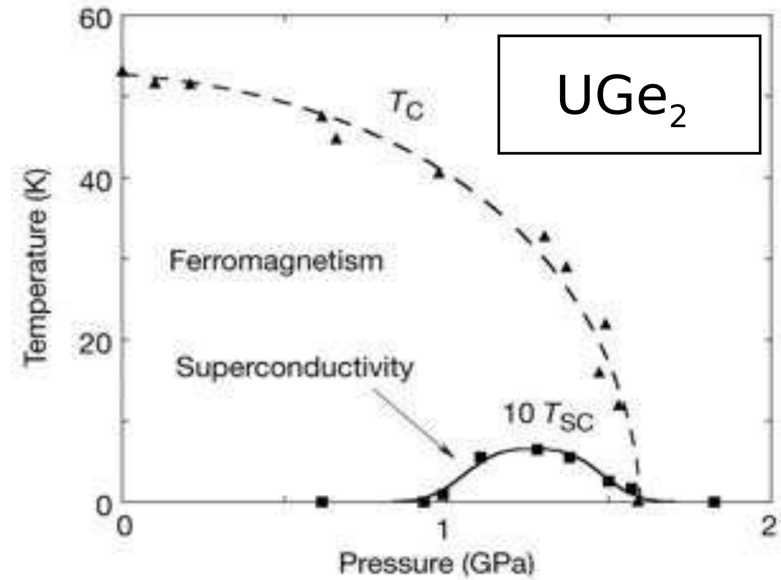

"Kondo breakdown"

"Avoided criticality"

Custers *et al*. Nature **424,** 524 (2003)

Julian *et al*. JPCM **8**, 9675 (1996)

Saxena *et al*. Nature **406,** 587 (2000)

Types of AFM quantum criticality (in HF systems)

Spin density wave type:

Assumes *f*-electrons to be hybridised with conduction band in both AFM and PM states

AFM ordered phase close to QCP can be described in terms of a spin density wave order of the heavy quasiparticles of the PM phase.

Changes in FS should be minor on crossing the QCP, and evolution of FS should be smooth.

Local criticality ("Kondo breakdown"):

Heavy quasiparticles break apart at the QCP on entering the AFM phase

f-electrons are decoupled from conduction electrons in ordered state and are effectively localised.

Must have abrupt change of FS size from "large" to "small" at the QCP.

Do all AFM heavy fermion QCPs fall into one of these two categories?

Quantum criticality in the SDW picture

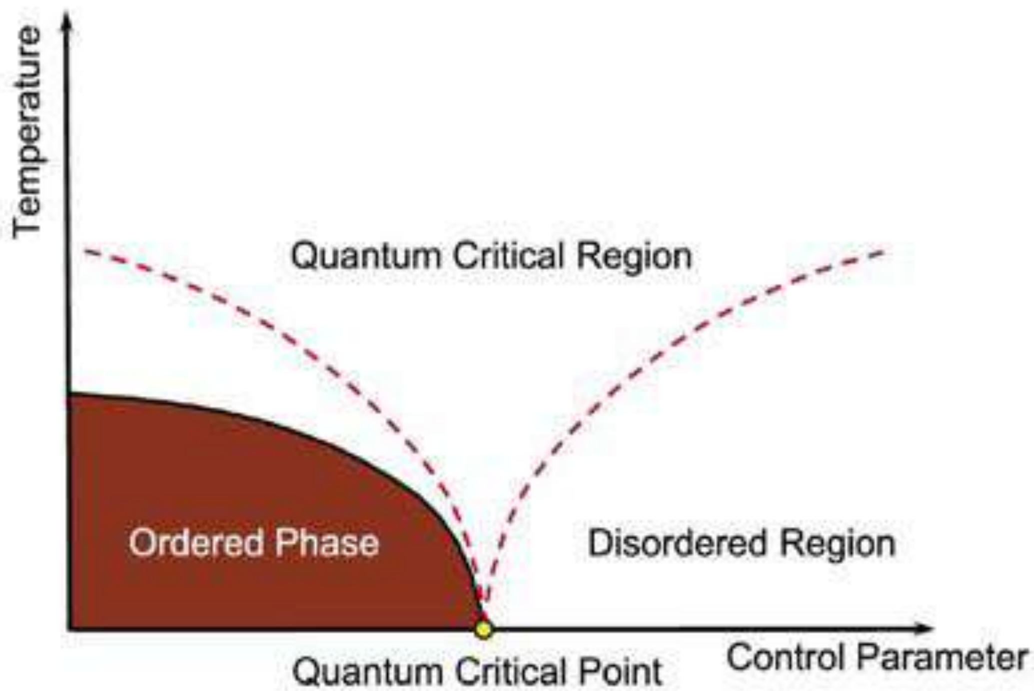

Landau approach (conventional quantum criticality):
phases distinguished by an order parameter which characterises spontaneous symmetry-breaking.

Quantum criticality described in terms of d+z dimensional fluctuations of the (AFM) order parameter (*d* is spatial dimension, *z* is the dynamical exponent).

Behaviour (scaling) should be predictable.

Q.Si, J.Phys.Soc.Jpn, **83**, 061005 (2014)

Local criticality and Kondo breakdown

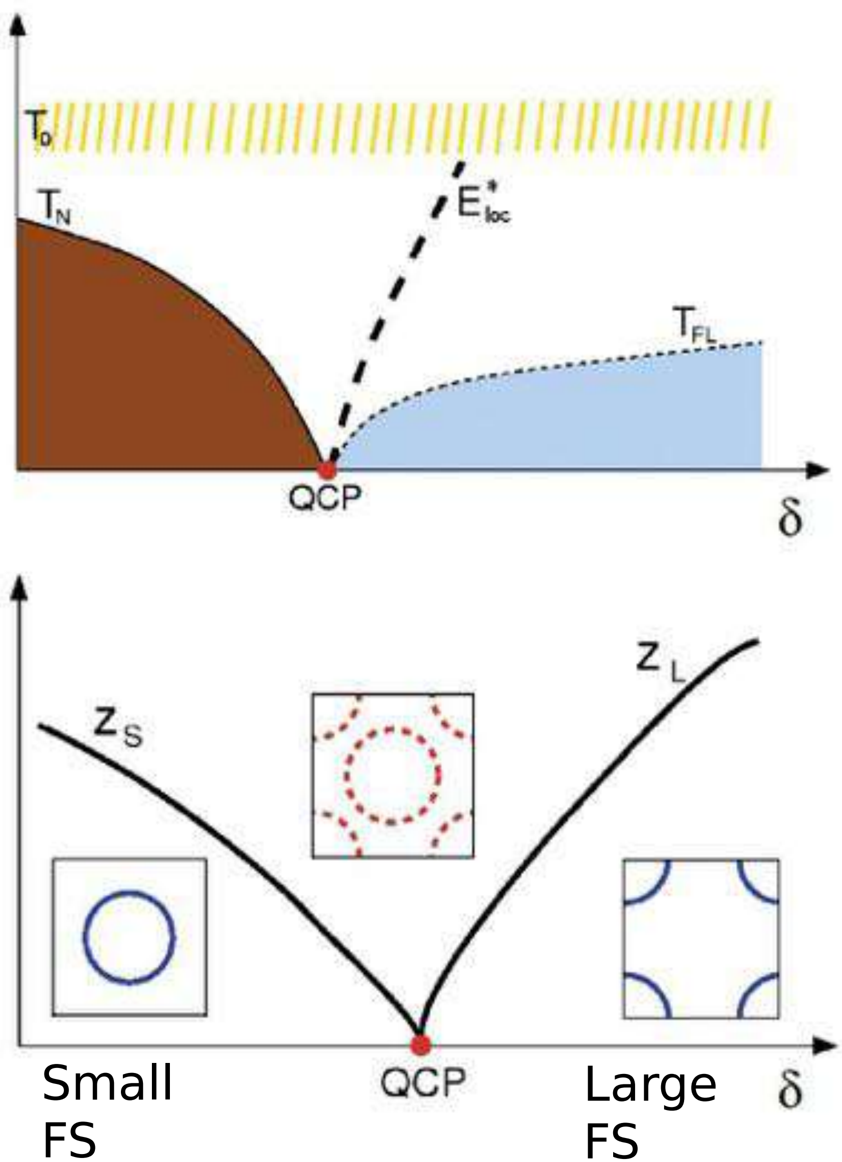

The QCP between AFM phase and PM heavy fermion state can show unusual dynamical scaling.

“**Local quantum criticality**” :
the *f*-electron is localised *at* the critical point.

New critical modes associated with breakdown of the Kondo effect (additional to fluctuations of the AFM order parameter).

The Fermi surface must change size when “Kondo breakdown” occurs.

Q.Si, J.Phys.Soc.Jpn, **83**, 061005 (2014)

The $CeM_m In_{3+2m}$ family

Bauer *et al*., PRB **81**, 180507(R) (2010)

Kurenbaeva *et al*., Intermetallics **16**, 979 (2008).
Tobash *et al*., JPCM **24**, 015601 (2012)

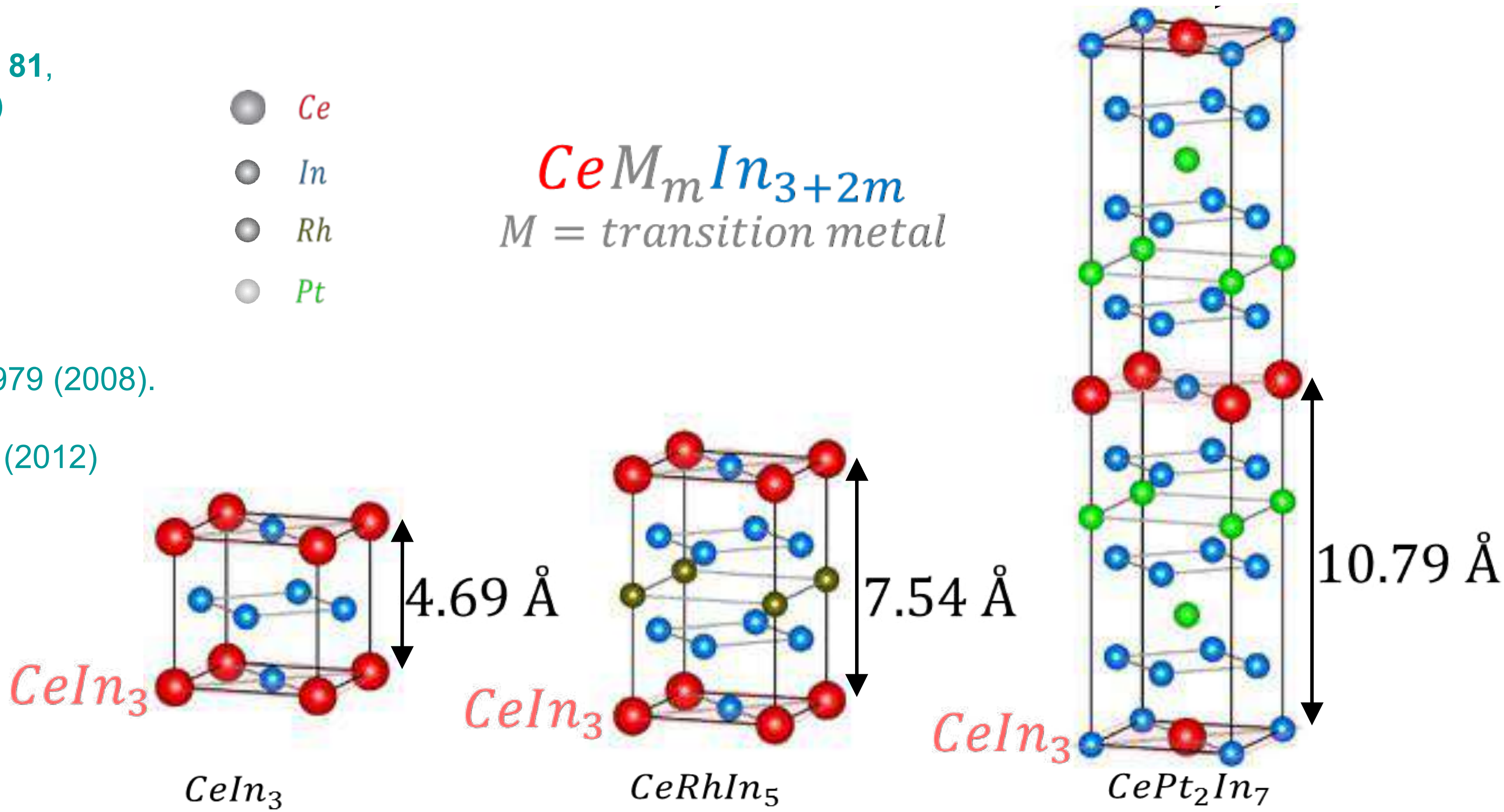

T_N = 10.1 K	T_N = 3.8 K	T_N = 5.5 K
P_c = 2.6 GPa	P_c = 2.4 GPa	P_c = 3.2-3.5 GPa
T_c = 0.17 K	T_c = 2.1 K	T_c = 2.1 K

superconductivity on suppression of T_N with pressure

Magnetic structure

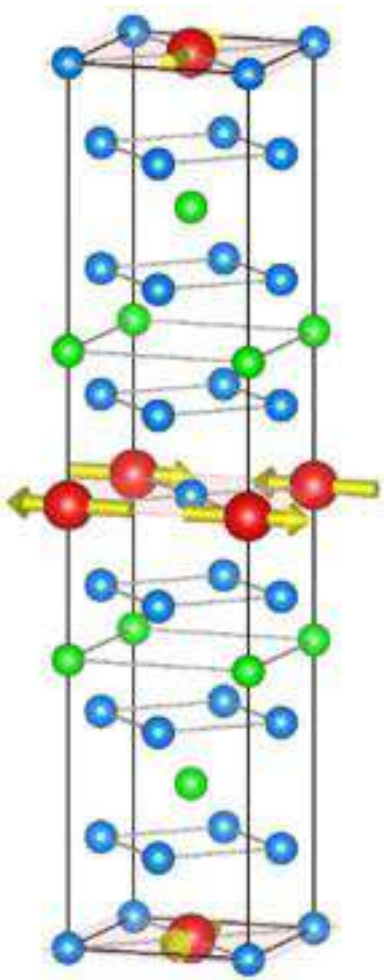

$CePt_2In_7$

Moments are in-plane along the *a*- or *b*-axis: $\vec{k} = \left(\frac{1}{2}, \frac{1}{2}, \frac{1}{2}\right)$

Moments: 0.45 μ_B/Ce at 2 K.

Moments rotate by 90° from one plane to another.

$CeIn_3$	$CeRhIn_5$
$\vec{k} = \left(\frac{1}{2}, \frac{1}{2}, \frac{1}{2}\right)$	$\vec{k} = \left(\frac{1}{2}, \frac{1}{2}, 0.297\right)$
$0.48\mu_B/Ce$	$0.75\mu_B/Ce$
180° from one plane to another	107° from one plane to another

Raba *et al.*, 95, 161102(R) (2017)

Phase diagrams

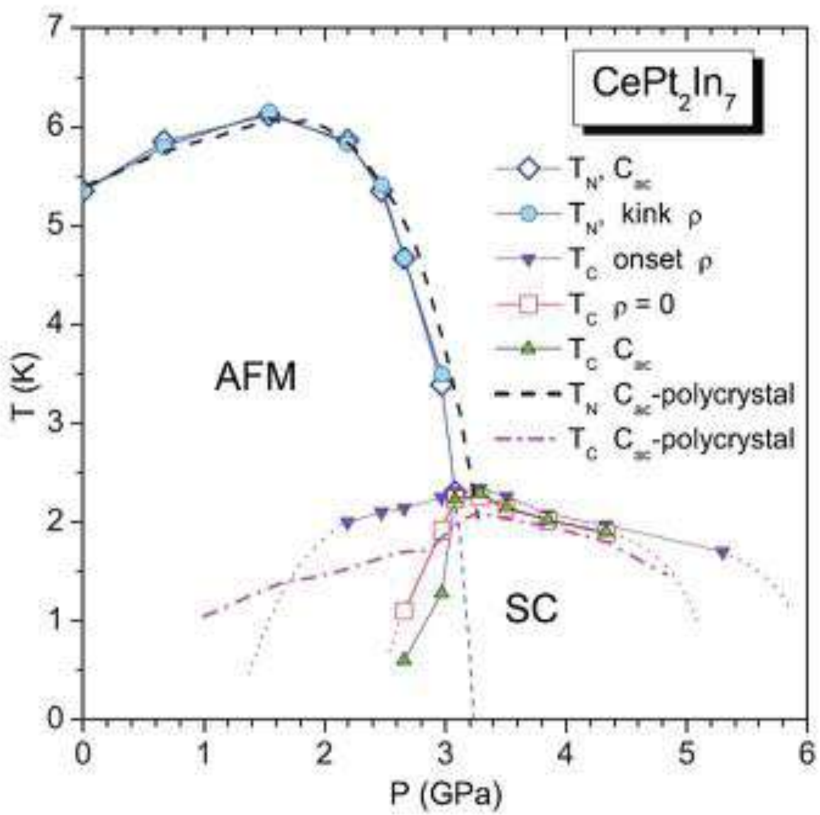

Sidorov *et al*., PRB **88**, 020503(R) (2013)

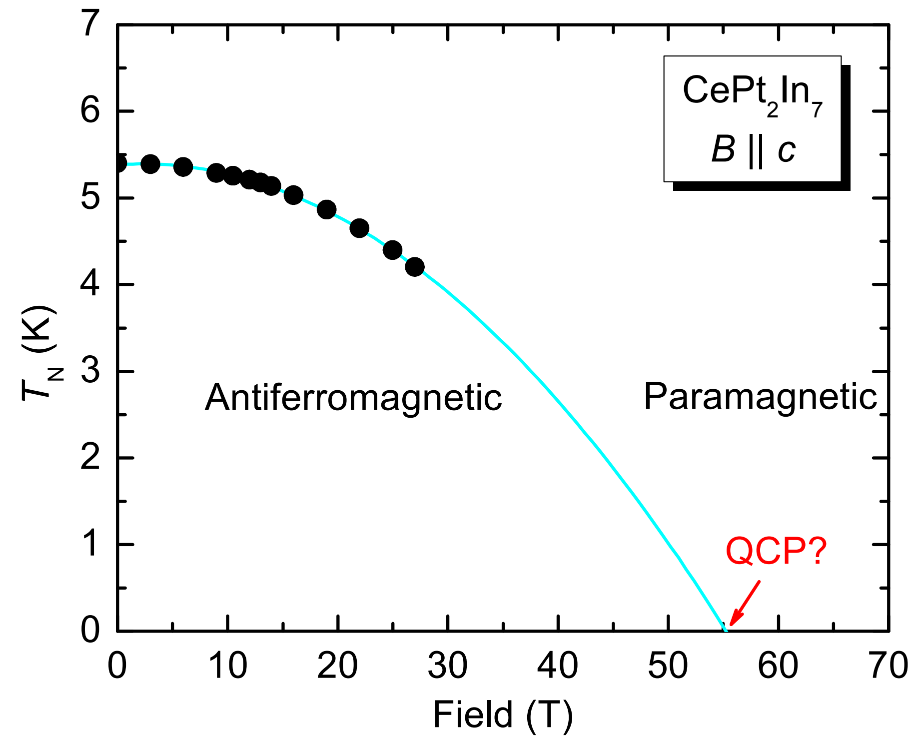

Krupko *et al*., PRB **93**, 085121 (2016)

2 quantum critical points:

suppression of AFM with pressure at ~ 3.2 GPa
suppression of AFM with magnetic field at ~ 55 T

Comparison with $CeIn_3$ and $CeRhIn_5$

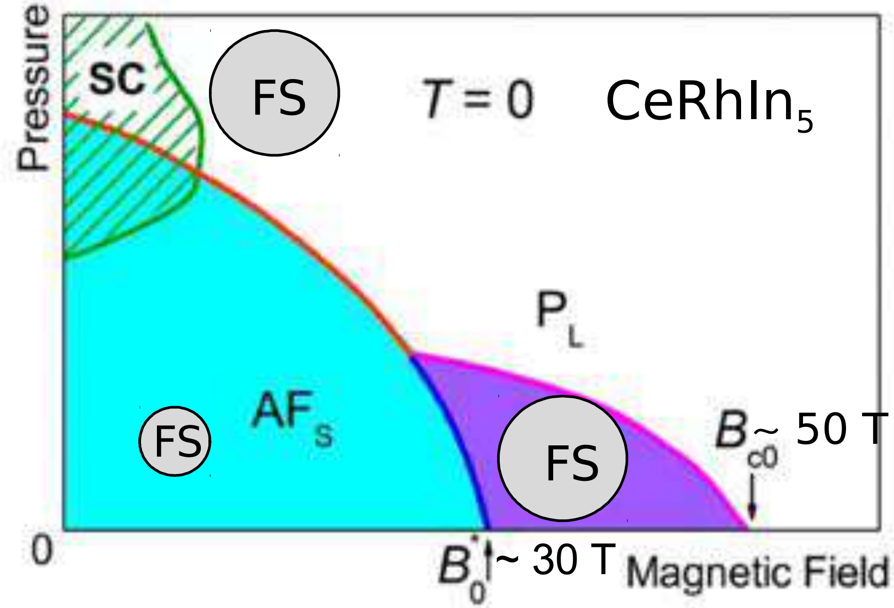

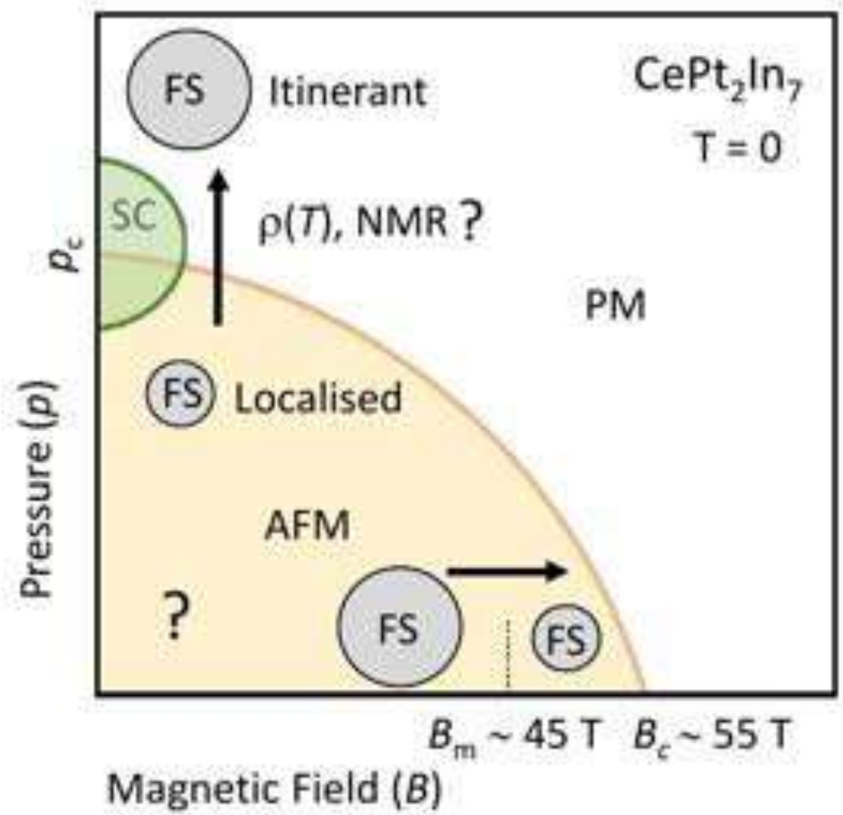

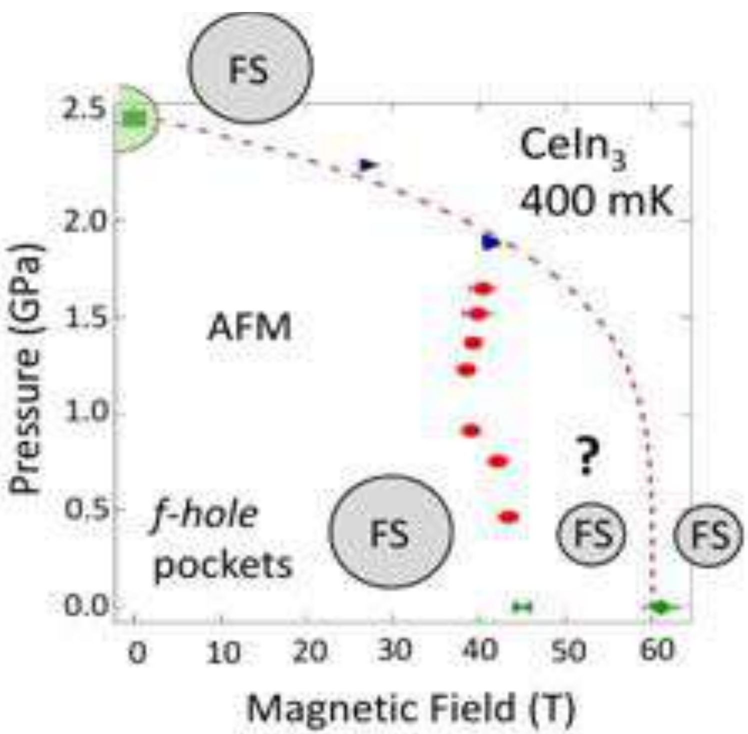

Shishido *et al*., JPSJ **74,** 1103 (2005)
Knebel *et al*., PRB **74**, 020501(R) (2006)
Jiao *et al*., PNAS **112**, 673 (2015)
Altarawneh *et al*., PRB **83**, 081103(R) (2011)
Sakai *et al*., PRL **112**, 206401 (2014)
Sidorov et al., PRB **88**, 020503(R) (2013)
Julian *et al*., JPCM **8**, 9675 (1996)
Harrison *et al*.,PRL **99**, 056401 (2007)
Purcell et al.,PRB **79**, 214428 (2009)

TDO measurements on $CePt_2In_7$

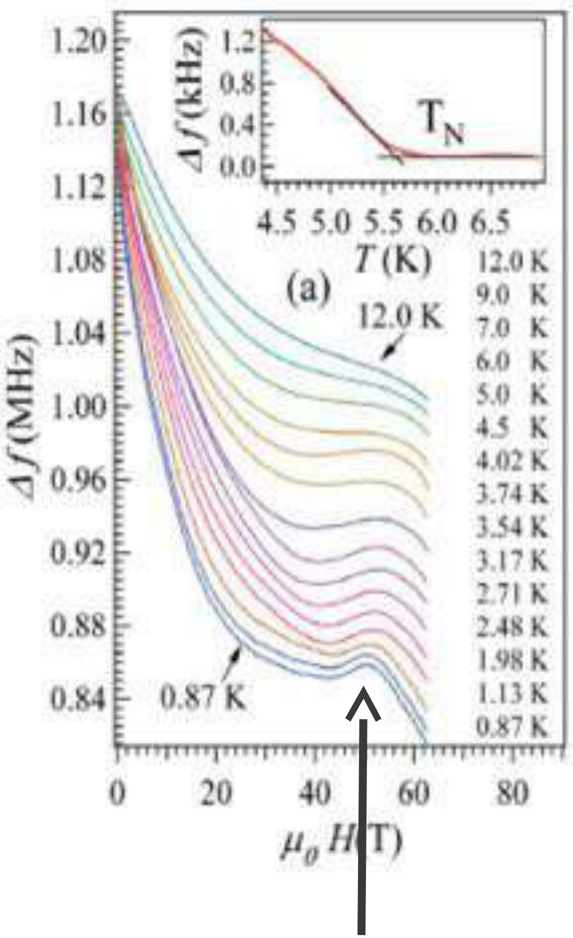

B_m ~ 45 T

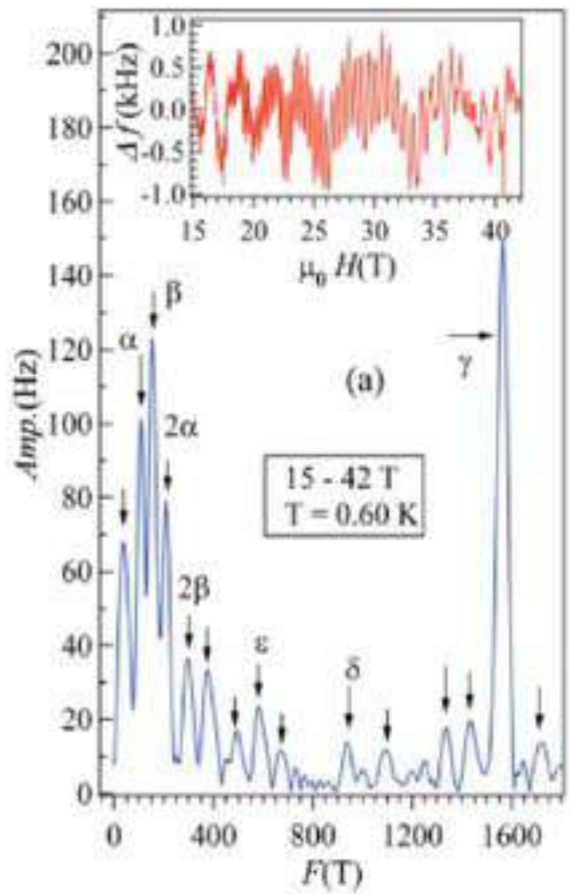

Many low frequencies with field-dependent m^*

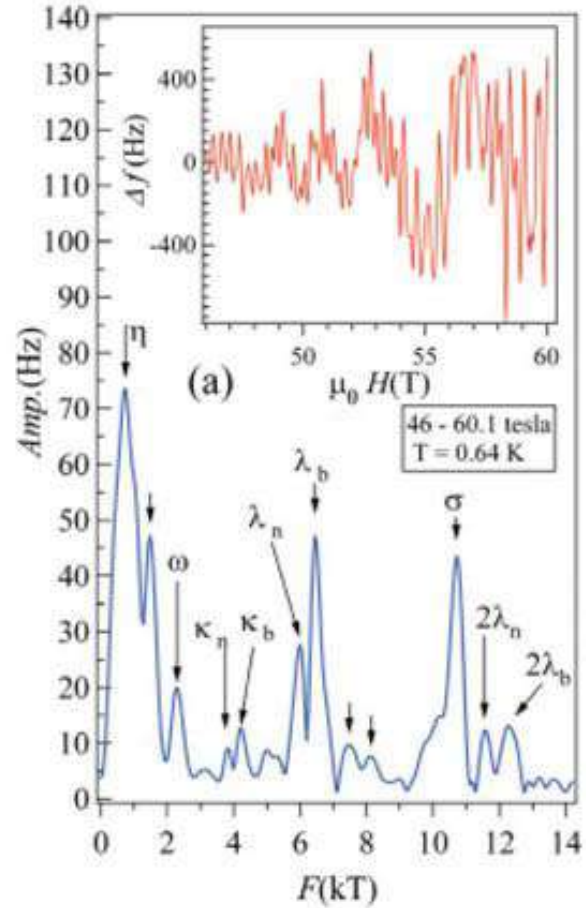

Higher frequencies appear above 45 T

Altarawneh *et al*., PRB **83**, 081103(R) (2011)

dHvA measurements via torque

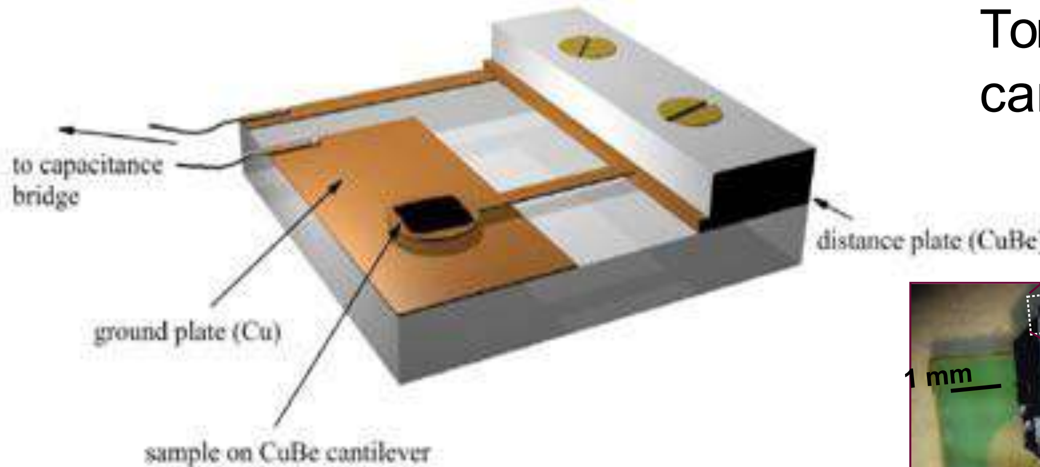

Torque measurements using a capacitive cantilever at LNCMI, Grenoble,

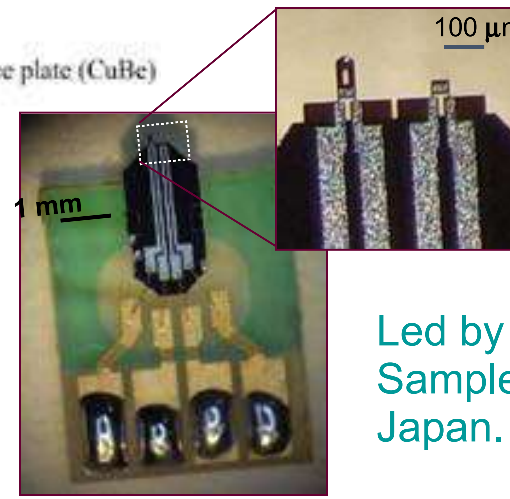

and a piezoresistive microcantilever at HFML, Nijmegen

Led by Ilya Sheikin, Grenoble, France. Samples grown by Rikio Settai, Niigata, Japan.

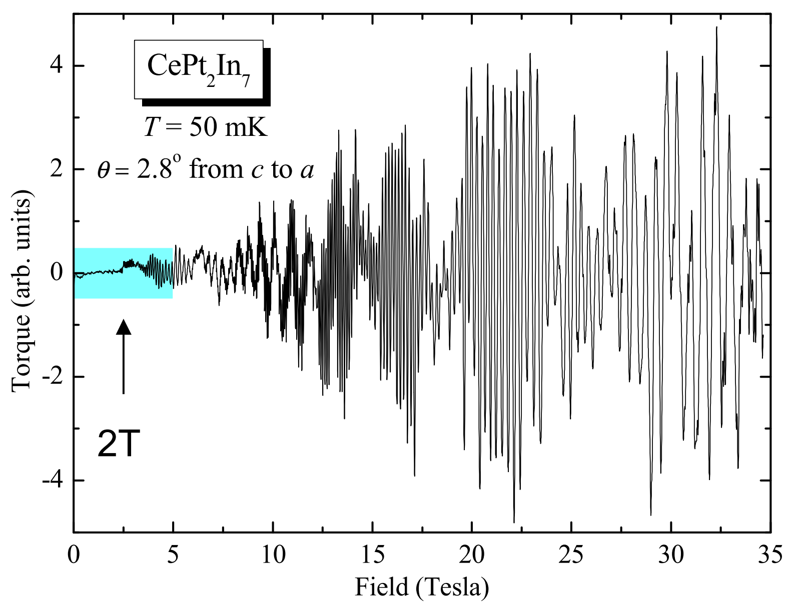

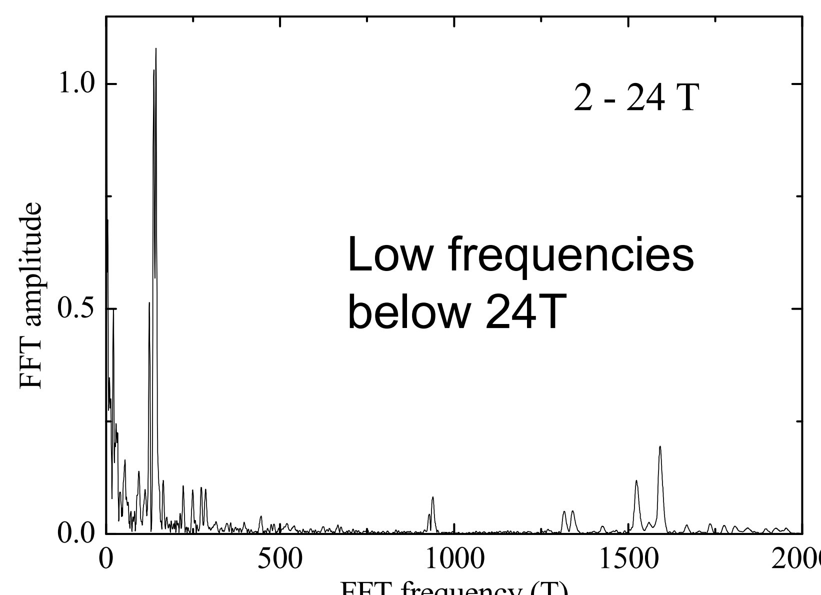

dHvA oscillations: B > 24 T

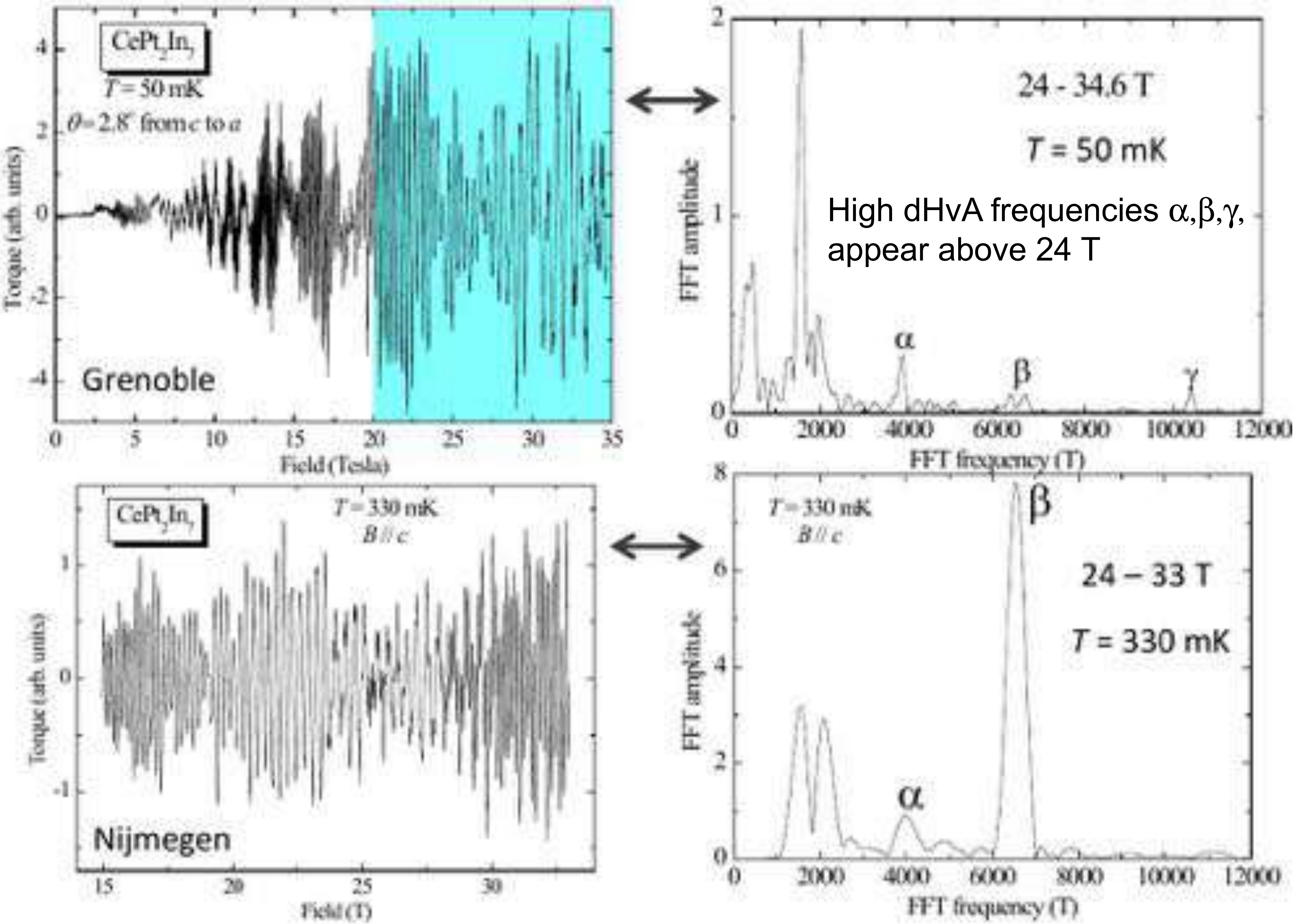

Effective masses

Three "high" dHvA frequencies from 24 T, suggesting no localisation transition (or Kondo breakdown) causing the disappearance of these frequencies at 45 T.

Quasiparticle effective masses relatively light, 2 m_e to 6 m_e. No strong field dependence.

f-electron always localised?

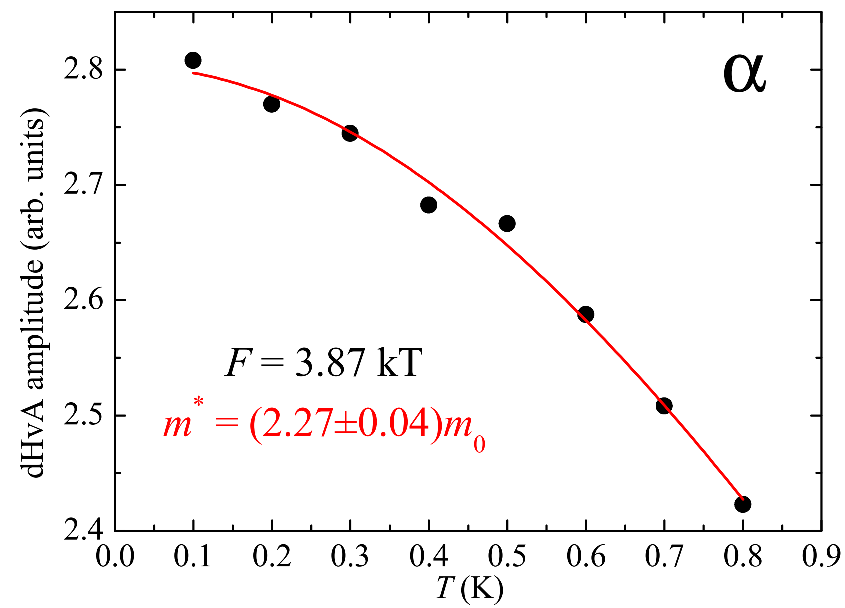

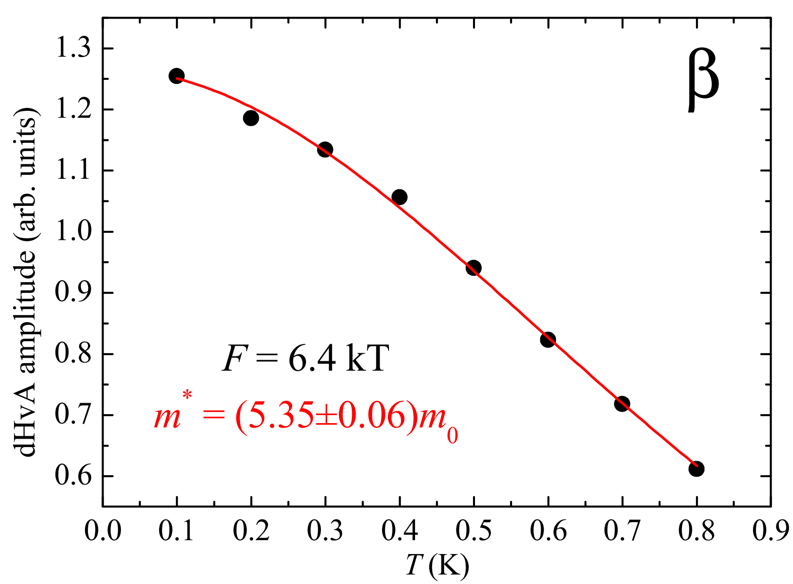

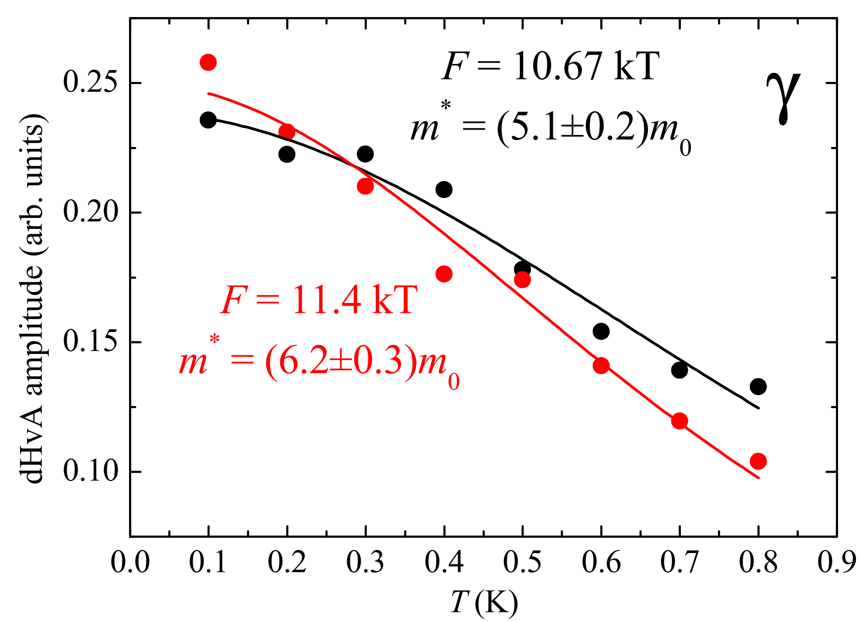

Bandstructure and Fermi surface calculations

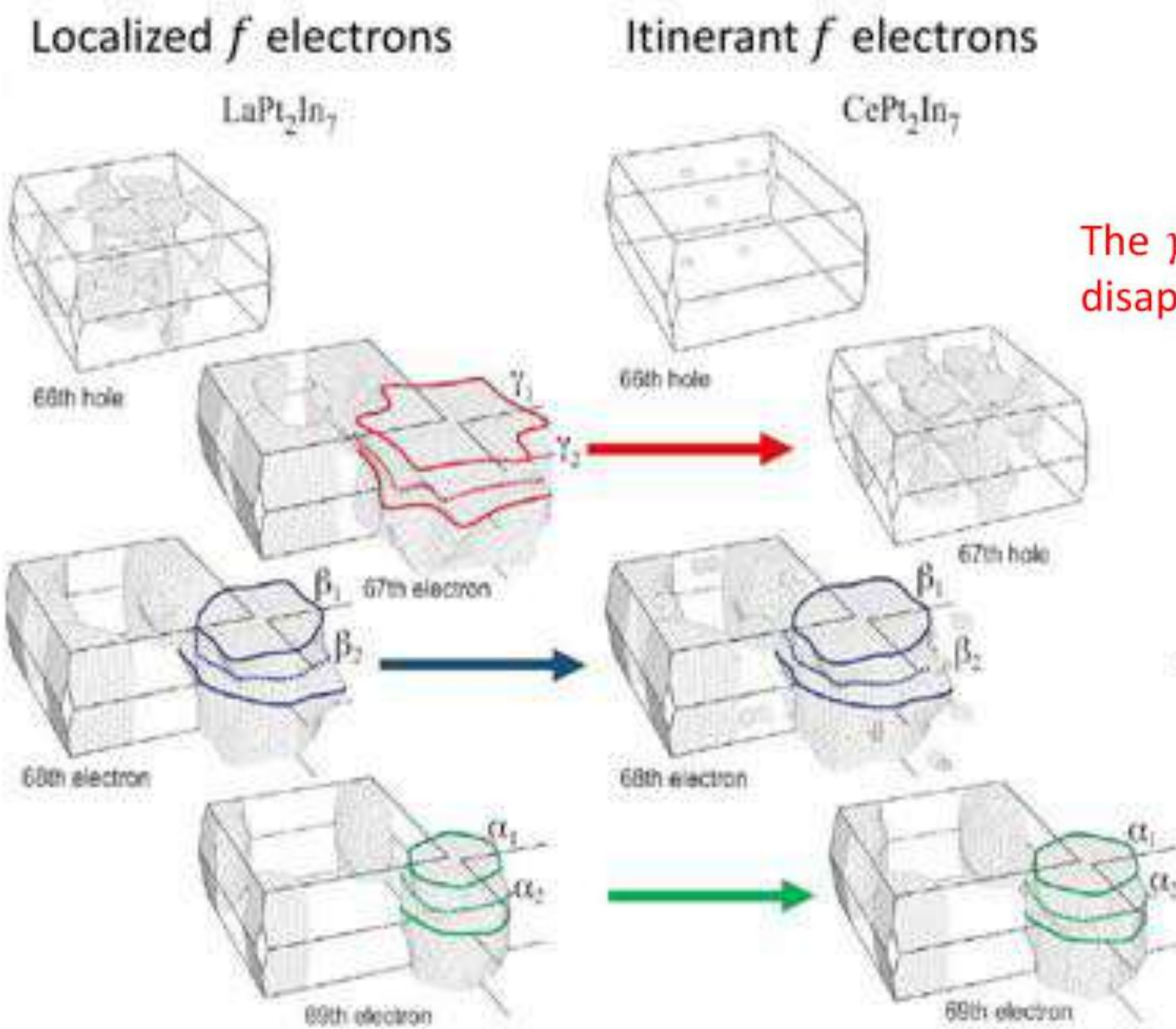

The γ frequency should disappear

The α and β frequencies should be shifted.

K. Götze et al., PRB **96**, 075138 (2017)

$CePt_2In_7$ Brillouin zone size

Why do we only see the α, β and γ frequencies above 24 T?

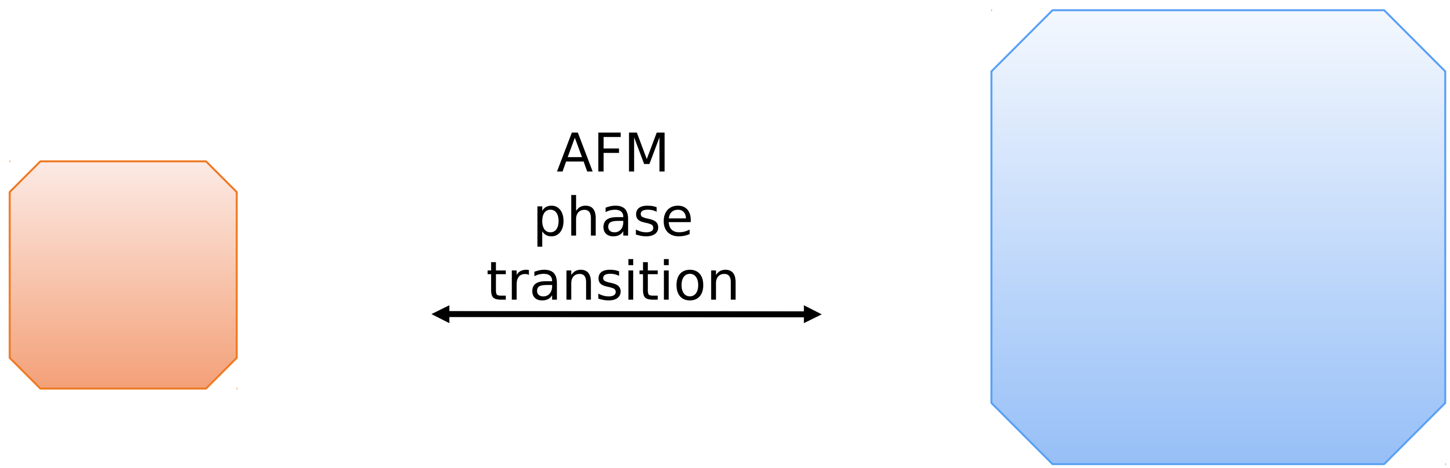

Magnetic Brillouin zone

Crystallographic Brillouin zone

Folding of Fermi surfaces → Need Magnetic breakdown (B > 25 T)

Angle dependence

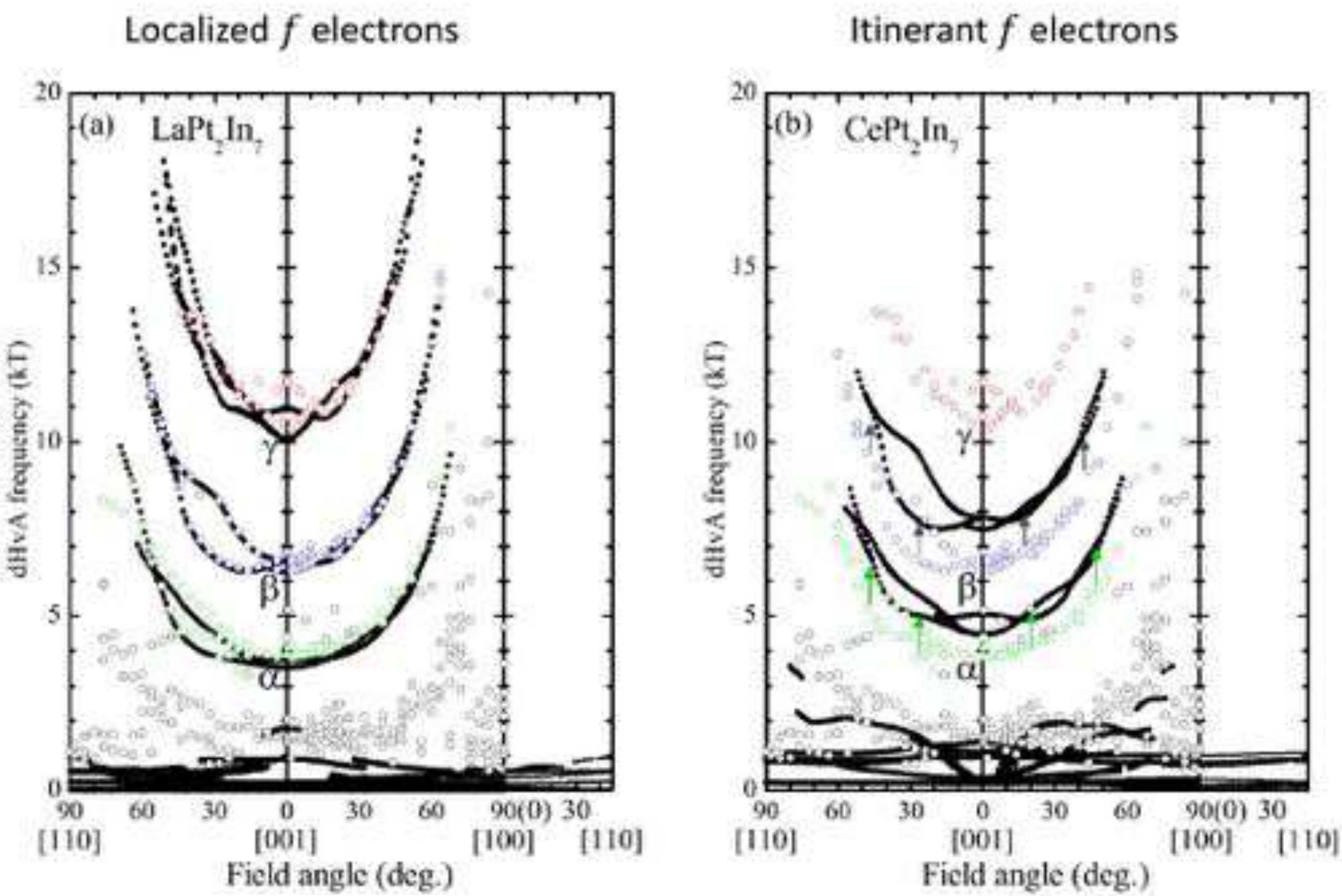

The γ frequency should disappear

The α and β frequencies should be shifted.

- Black: calculation

○ Color: dHvA experiment results up to 35 T .

Non-magnetic analogue

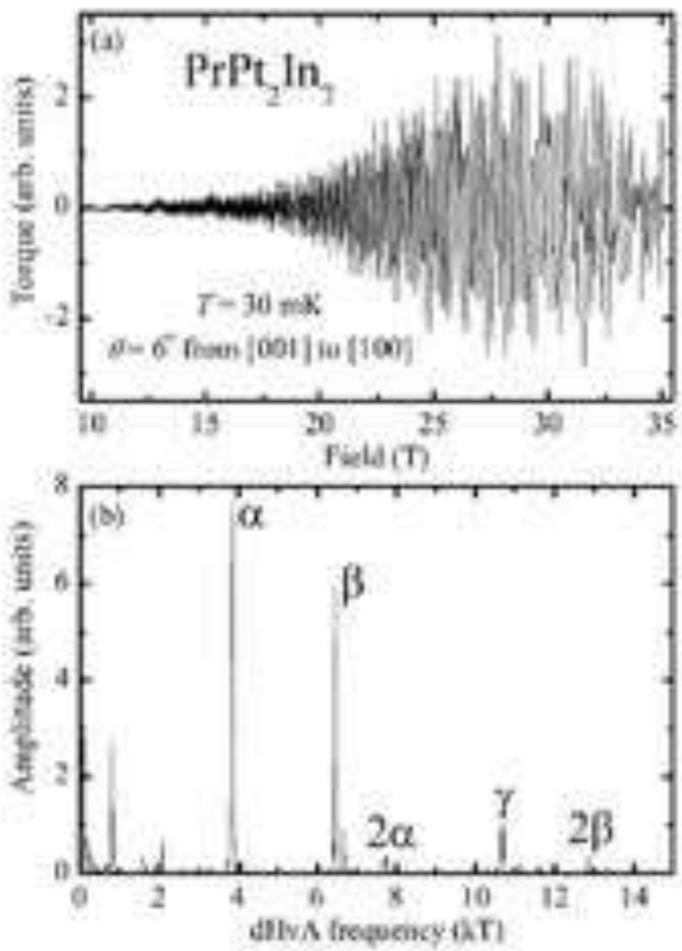

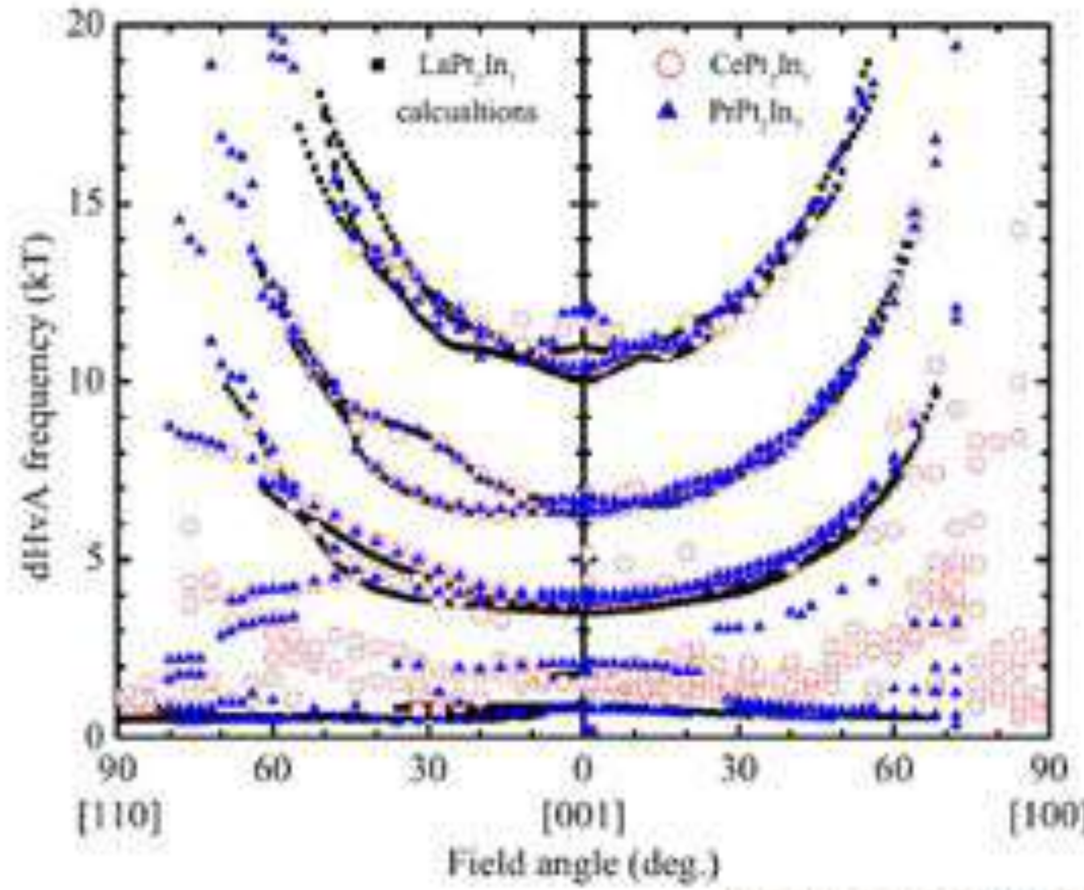

K. Götze *et al.*, PRB **96**, 075138 (2017)

$PrPt_2In_7$ has no *f*-electron in Fermi volume, and data look almost identical to data for $CePt_2In_7$

Pulsed field measurements

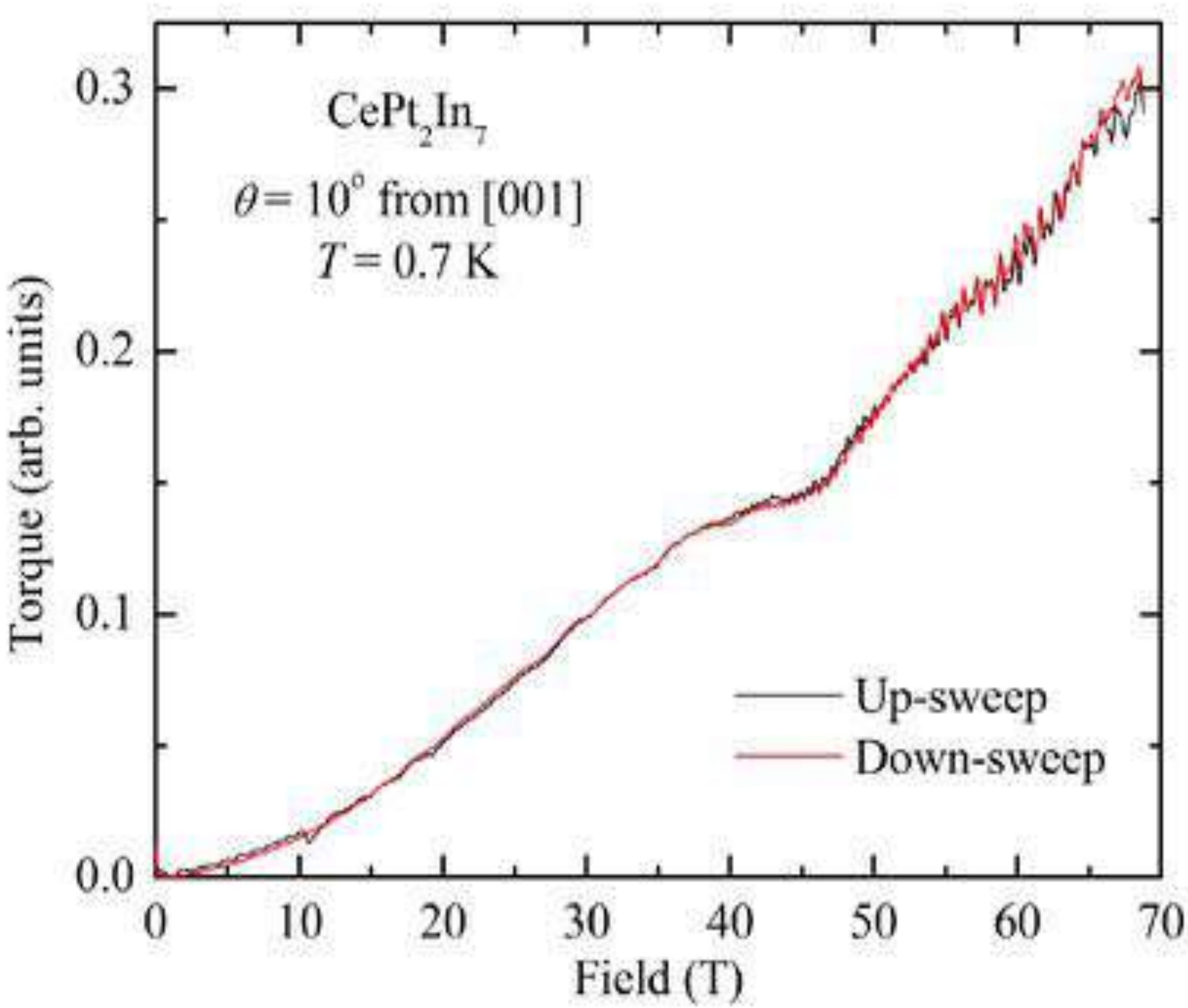

Clear feature at ~ 45 T, but no change of FS across this region.

Localised *f*-electrons up to 70 T

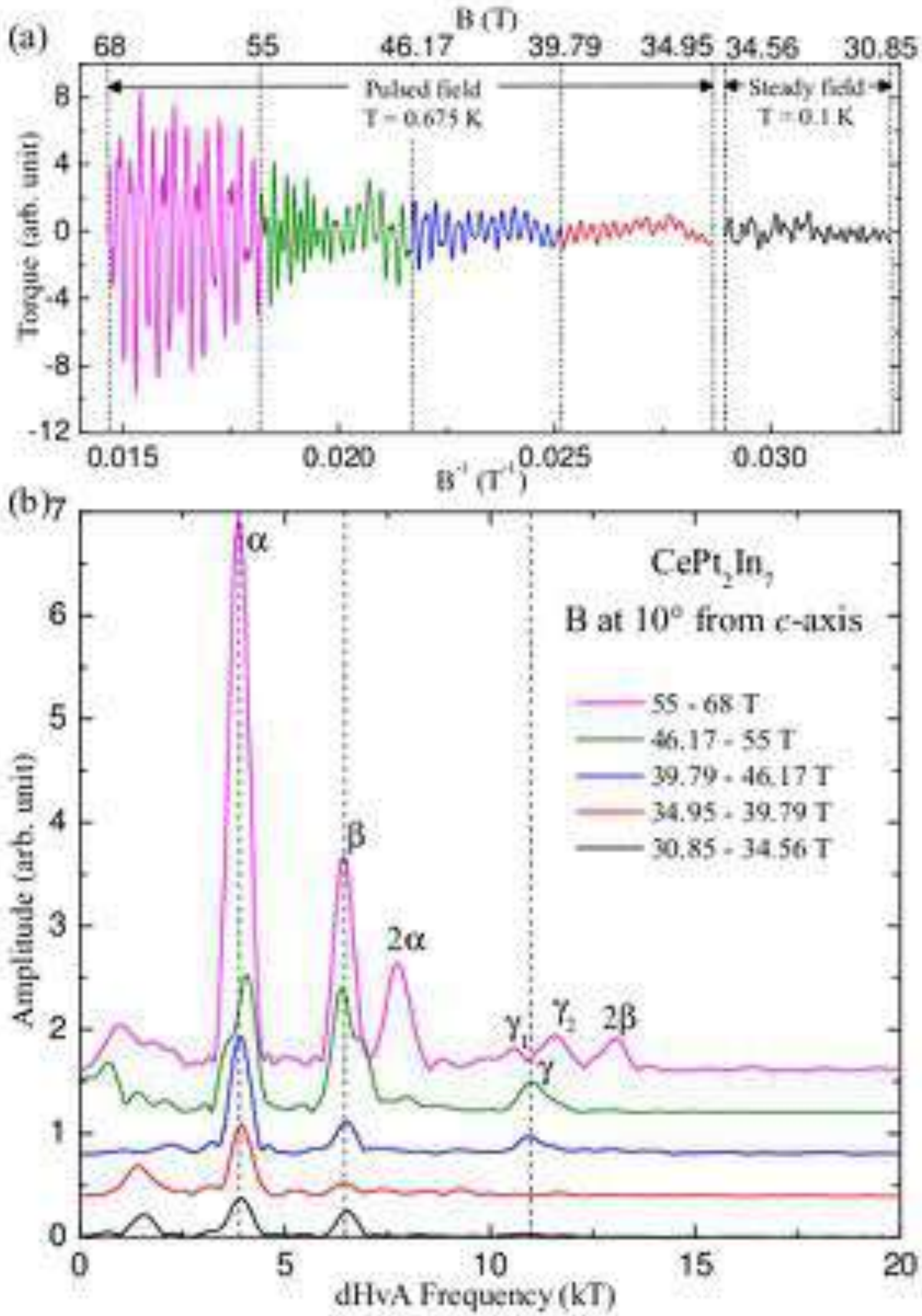

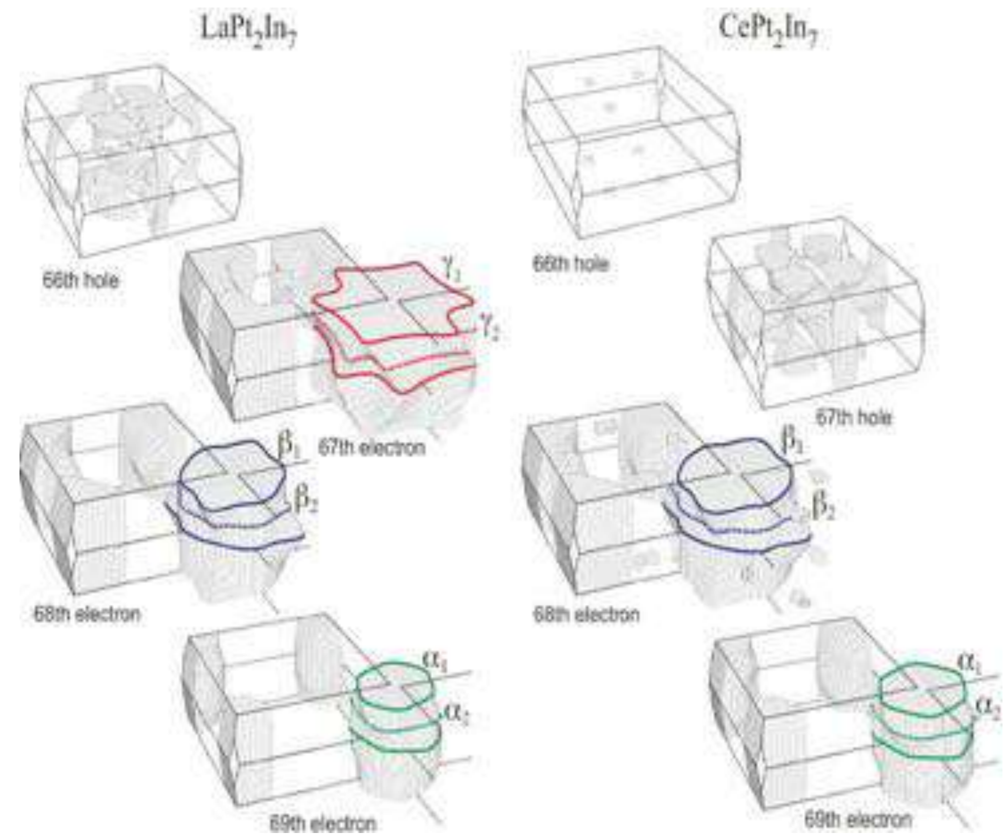

High field feature

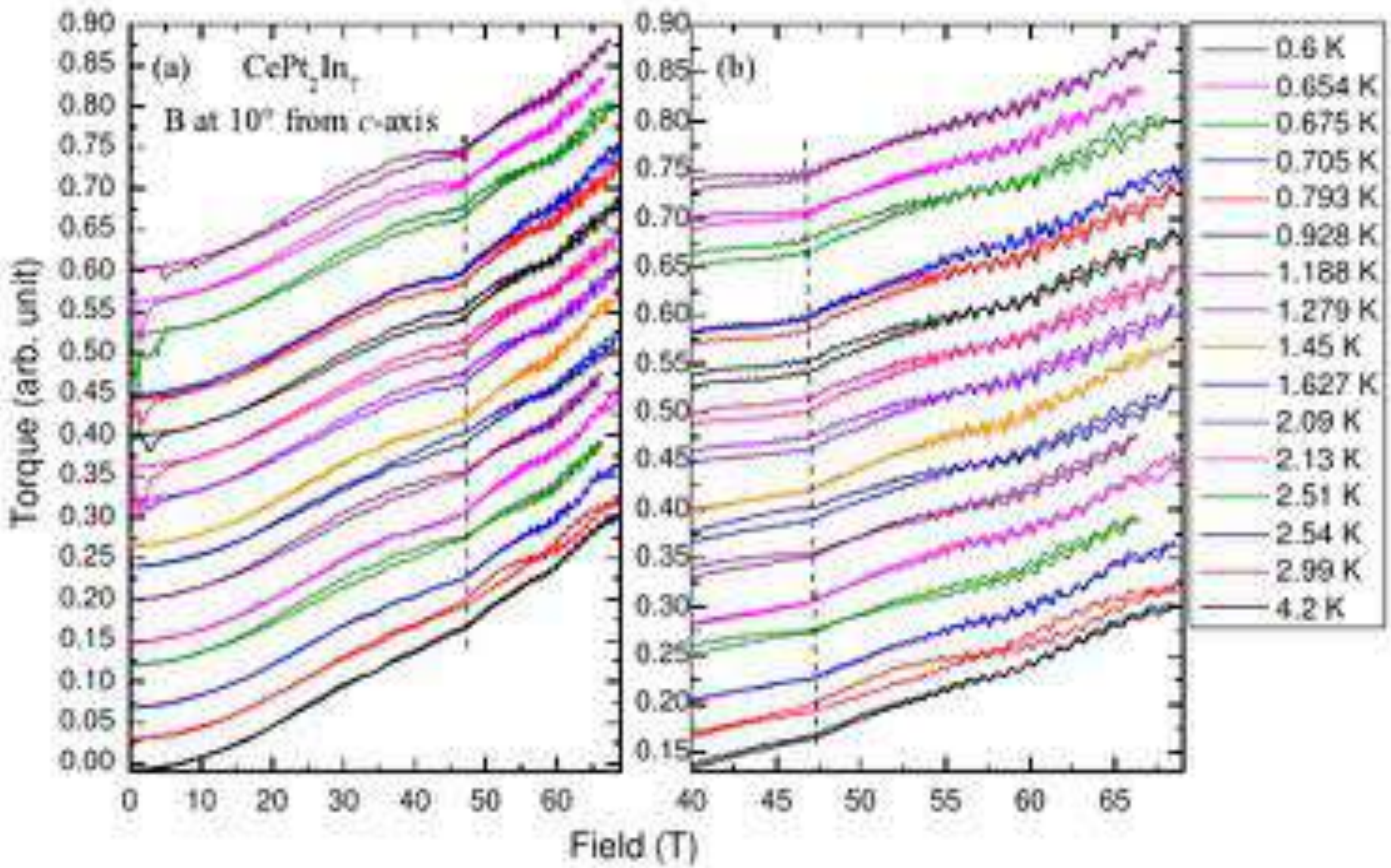

Valence transition

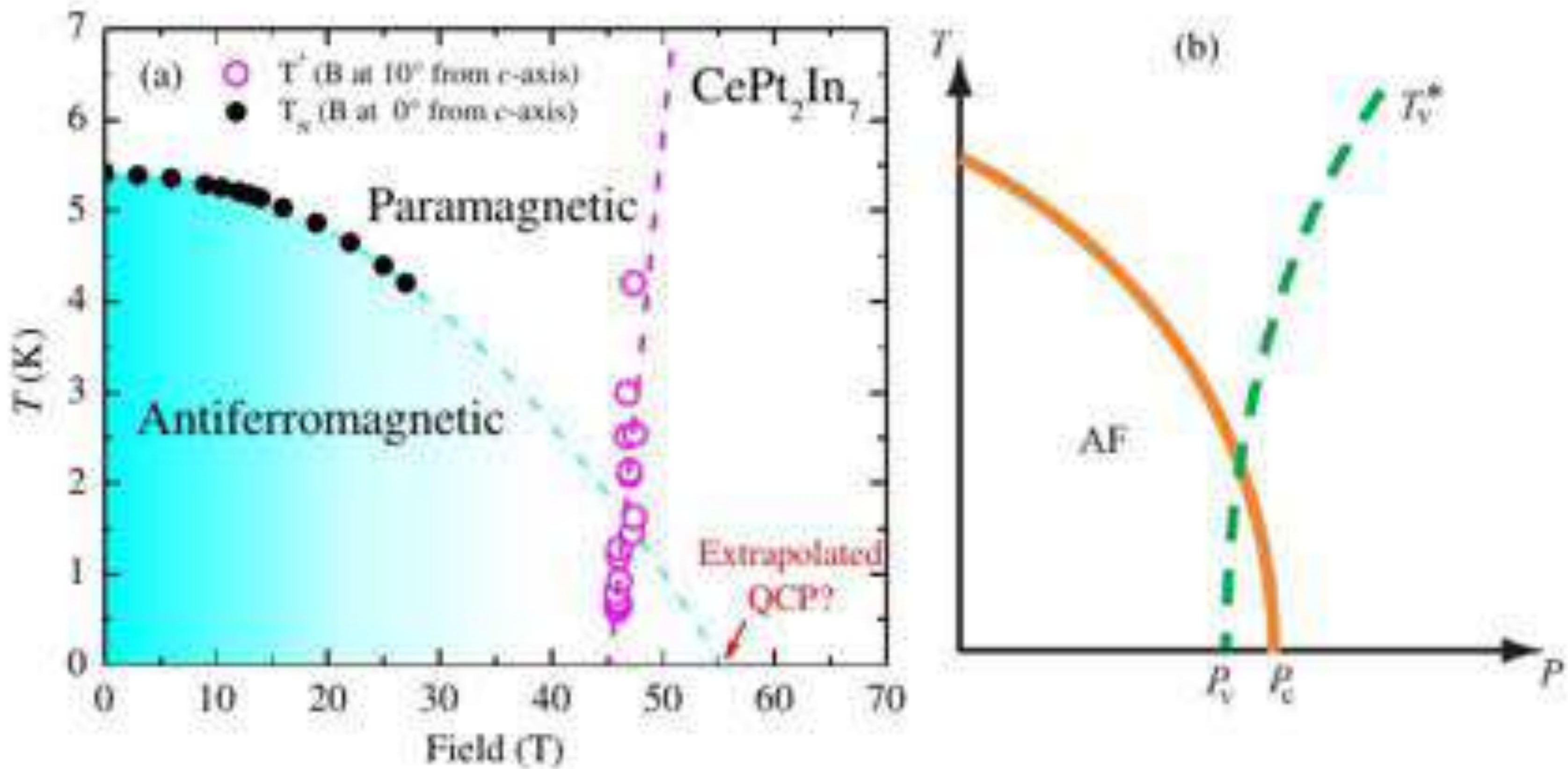

Watanabe and Miyake, JPCM **23**, 094219 (2011)

Watanabe and Miyake, JPCM **24**, 294208 (2012)

M. Raba. PhD Thesis. Université Grenoble Alpes (2018)

Change of effective mass

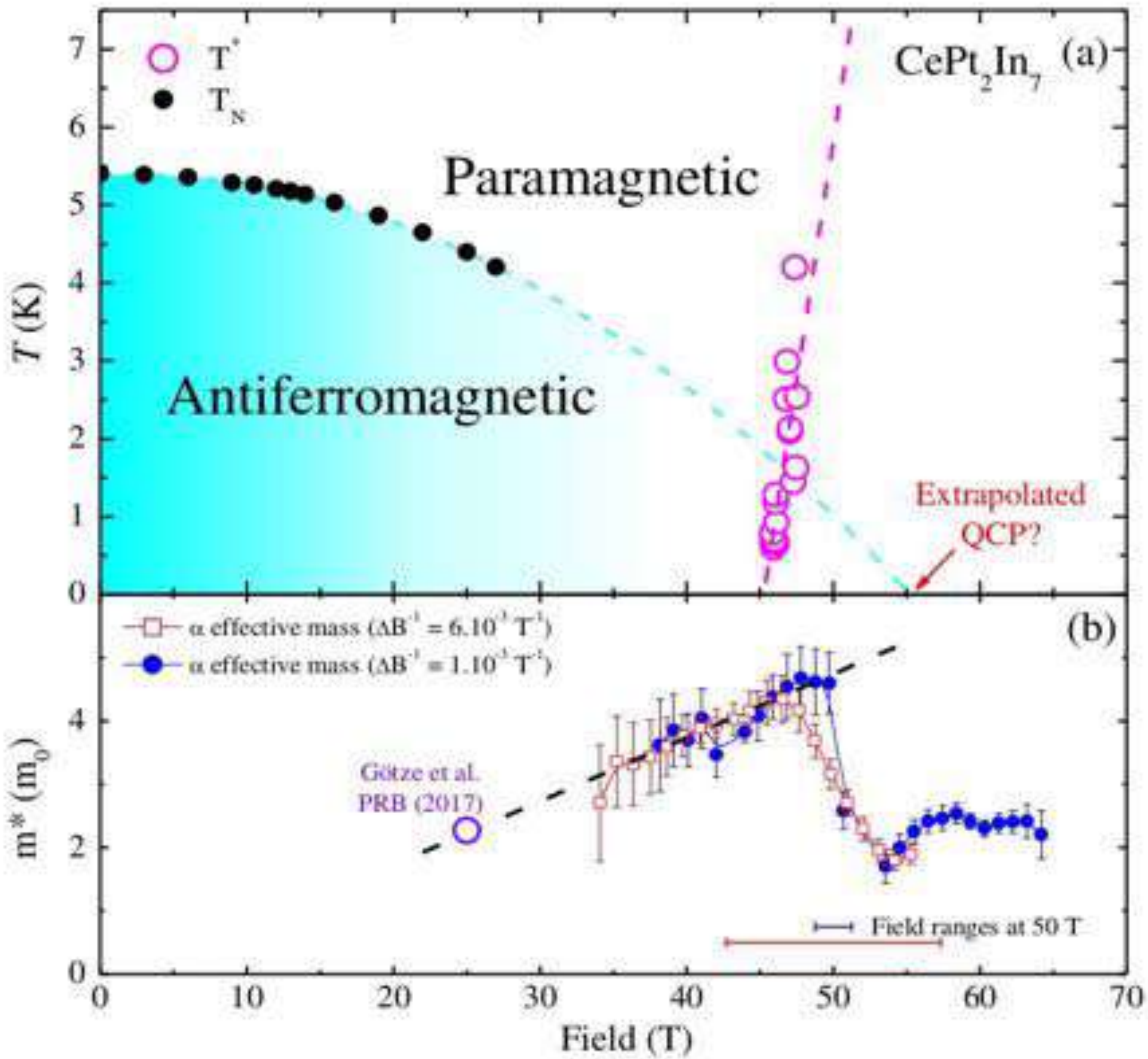

In summary

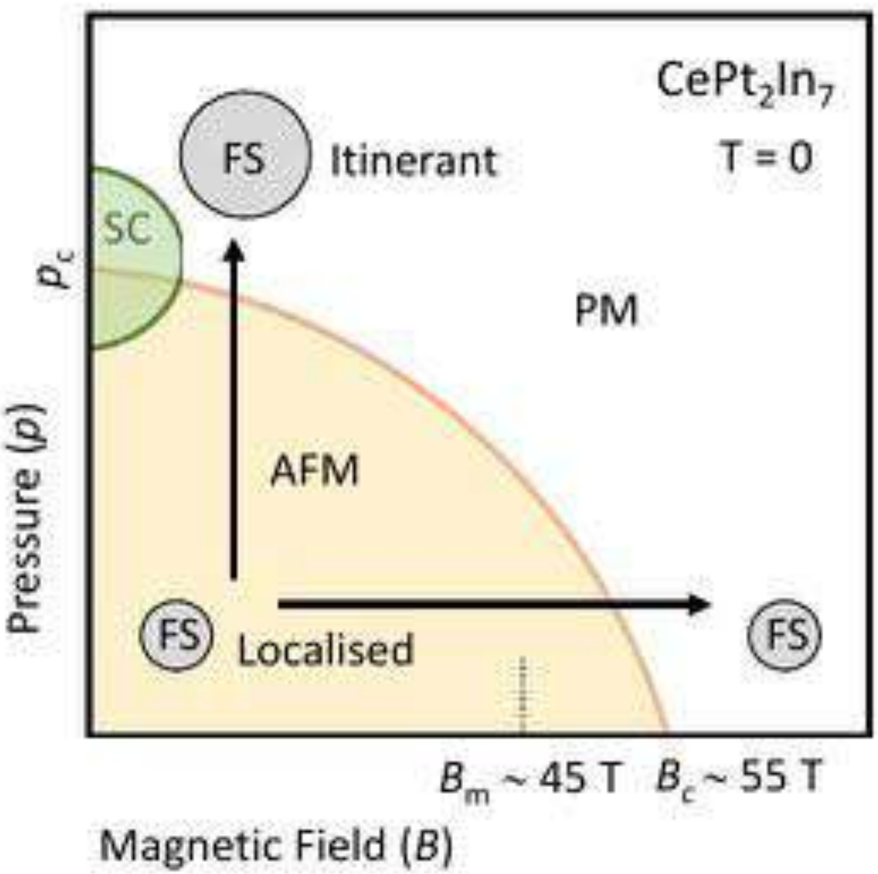

dHvA measurements show that *f*-electrons are localised (at ambient pressure) in $CePt_2In_7$ to fields as high as 70 T.

No dramatic change of FS across field suppression of AFM.

Valence transition associated with 45 T feature.